HELDA
HELSINGIN YLIOPISTO
HELSINGFORS UNIVERSITET
UNIVERSITY OF HELSINKI

UNIVERSITY OF HELSINKI

https://helda.helsinki.fi

Temporal transcriptome analysis of the white-rot fungus Obba rivulosa shows expression of a constitutive set of plant cell wall degradation targeted genes during growth on solid spruce wood

Marinovic, Mila

2018-03

Marinovic , M , Aguilar-Pontes , M V , Zhou , M , Miettinen , O K , de Vries , R , Mäkelä , M R & Hilden , S K 2018 , ' Temporal transcriptome analysis of the white-rot fungus Obba rivulosa shows expression of a constitutive set of plant cell wall degradation targeted genes during growth on solid spruce wood ' , Fungal Genetics and Biology , vol. 112 , pp. 47-54 . https://doi.org/10.1016/j.fg

http://hdl.handle.net/10138/327006
https://doi.org/10.1016/j.fgb.2017.07.004

cc_by_nc_nd
acceptedVersion

Downloaded from Helda, University of Helsinki institutional repository.

This is an electronic reprint of the original article.

This reprint may differ from the original in pagination and typographic detail.

Please cite the original version.

Temporal transcriptome analysis of the white-rot fungus *Obba rivulosa* shows expression of a constitutive set of plant cell wall degradation targeted genes during growth on solid spruce wood

Mila Marinović[a], Maria Victoria Aguilar-Pontes[b,c], Miaomiao Zhou[b,c], Otto Miettinen[d], Ronald P. de Vries[a,b,c], Miia R. Mäkelä[a], Kristiina Hildén[a#]

[a]Division of Microbiology and Biotechnology, Department of Food and Environmental Sciences, University of Helsinki, Viikinkaari 9, Helsinki, Finland

[b]Westerdijk Fungal Biodiversity Institute, Uppsalalaan 8, 3584 CT Utrecht, The Netherlands

[c]Fungal Molecular Physiology, Utrecht University, Uppsalalaan 8, 3584 CT Utrecht, The Netherlands

[d]Finnish Museum of Natural History, University of Helsinki, Helsinki, Finland

#Corresponding author: email: kristiina.s.hilden@helsinki.fi

Abstract

The basidiomycete white-rot fungus *Obba rivulosa*, a close relative of *Gelatoporia* (*Ceriporiopsis*) *subvermispora*, is an efficient degrader of softwood. The dikaryotic *O. rivulosa* strain T241i (FBCC949) has been shown to selectively remove lignin from spruce wood prior to depolymerization of plant cell wall polysaccharides, thus possessing potential in biotechnological applications such as pretreatment of wood in pulp and paper industry. In this work, we studied the time-course of the conversion of spruce by the genome-sequenced monokaryotic *O. rivulosa* strain 3A-2, which is derived from the dikaryon T241i, to get insight into transcriptome level changes during prolonged solid state cultivation. During 8-week cultivation, *O. rivulosa* expressed a constitutive set of genes encoding putative plant cell wall degrading enzymes. High level of expression of the genes targeted towards all plant cell wall polymers was detected at 2-week time point, after which majority of the genes showed reduced expression. This implicated non-selective degradation of lignin by the *O. rivulosa* monokaryon and suggests high variation between mono- and dikaryotic strains of the white-rot fungi with respect to their abilities to convert plant cell wall polymers.

Keywords

Obba rivulosa; white-rot; lignocellulose; solid state cultivation; transcriptomics

Abbreviations

AA, auxiliary activity; AAO, aryl alcohol oxidase; AE, acetylesterase; AGL, α-galactosidase; AGU, α-glucuronidase; AOX, alcohol oxidase; BGL, β-1,4-glucosidase; CAZy, CAZyme, carbohydrate-active enzyme; CBH, cellobiohydrolase; CDH, cellobiose dehydrogenase; CE, carbohydrate esterase; CRO, copper radical oxidase; EGL, β-1,4-edoglucanase; ENO, enolase; FBA, fructose-bisphosphate aldolase; FET, ferroxidase; FPKM, Fragments Per Kilobase of exon model per Million fragments mapped; GAL,

β-1,4-endogalactanase; GE, 4-O-methyl-glucuronyl methylesterase, glucuronoyl esterase; GH, glycoside hydrolase; GLX, glyoxal oxidase; GMC, oxidoreductase glucose-methanol-choline oxidoreductase; GND, 6-phosphogluconate dehydrogenase; GOX, glucose (1-)oxidase; GPD, glyceraldehyde-3-phosphate dehydrogenase; GT, glycosyl transferase; ICL, isocitrate lyase; LAR, L-arabinose reductase; LCC, laccase; LiP, lignin peroxidase; LN-AS, low nitrogen-asparagine-succinate; LPMO, lytic polysaccharide monooxygenase; MAN, β-1,4-endomannanase; MB, mega base pairs; MDH, malate dehydrogenase; MEA, malt extract agar; MND, β-1,4-mannosidase; MnP, manganese peroxidase; OXA, oxaloacetase; PCA, principal component analysis; PCP, pentose catabolic pathway;, PCWDE, plant cell wall degrading enzyme; PFK, fructose-2,6-bisphosphatase; PGA, endopolygalacturonase; PGI, glucose-6-phosphate isomerase; PKI, pyruvate kinase; PL, polysaccharide lyase; PPP, pentose phosphate pathway; qRT-PCR, quantitative real-time PCR; RNA-seq, RNA sequencing; TAL, transaldolase; TCA cycle, tricarboxylic acid cycle; VP, versatile peroxidase; XDH, xylitol dehydrogenase; XG-EG, xyloglucanase, xyloglucan-active endoglucanase; XLN, β-1,4-endoxylanase

1. Introduction

Plant biomass, as the most abundant renewable carbon source on Earth, is important not only for carbon cycling, but also as a feedstock for biofuels and newly derived value-added products (Isikgor and Becer, 2015). The main polymeric components comprising the plant cell wall, i.e. cellulose, hemicellulose, lignin and pectin, are responsible for its structural complexity. However, recalcitrance of lignocellulose is mostly due to the amorphous aromatic polymer lignin and presents the biggest obstacle in biotechnological exploitation of plant biomass.

Although a variety of microorganisms can attack lignocellulose, white-rot basidiomycete fungi are the most effective plant cell wall degrading organisms as they efficiently decompose all lignocellulose components by a variety of extracellular enzymes (Hatakka and Hammel, 2011; Mäkelä et al., 2014). Major cell wall polymers are being degraded by action of extracellular hydrolytic and oxidative enzymes, most of which have been categorized in the database of Carbohydrate-Active EnZymes (CAZy, http://www.cazy.org/) (Lombard et al., 2013). The resulting monomeric sugars are taken up by the fungal cells and metabolized as carbon and energy sources through specific pathways (Khosravi et al., 2015).

Lignin degradation is a prerequisite for gaining access to carbohydrate polymers, which serve as a carbon and energy source for fungi (Rytioja et al., 2014). White-rot fungi produce an array of oxidoreductases from the families of auxiliary activities (AA) that are known to take part in lignin modification and degradation. Of those, the key enzymes are fungal class II peroxidases, i.e. lignin peroxidases (LiPs), manganese peroxidases (MnPs) and versatile peroxidases (VPs) that are present in all efficient lignin degrading white-rot fungi in different numbers. In addition, laccases that are phenol-oxidizing multicopper oxidases are suggested to participate in lignin conversion with peroxidases in the presence of the aromatic mediator molecules (Zhao et al., 2016). Moreover, several extracellular H_2O_2-generating enzymes are a part of ligninolytic system (Ferreira et al., 2015). These include glucose-methanol-choline (GMC) enzymes alcohol oxidases (AOXs), aryl alcohol oxidases, (AAOs) glucose 1-oxidases (GOXs), and copper radical oxidases (CROs) such as glyoxal oxidases (GLXs). White-rot fungi are able to completely depolymerize the plant cell wall polysaccharides by secreting various hydrolytic enzymes, including cellulases and hemicellulases, from several glycoside hydrolase (GH) families (Rytioja et al., 2014). Besides hydrolytic enzymes, lytic polysaccharide monooxygenases

(LPMOs) and cellobiose dehydrogenases (CDHs) facilitate degradation of plant cell wall polysaccharides by oxidative action (Vaaje-Kolstad et al., 2010; Langston et al., 2011).

Wood decay patterns differ among white-rot fungi (Cantarel et al., 2008). Most of the studied species, including the model white-rot fungus *Phanerochaete chrysosporium*, remove cellulose, hemicellulose and lignin simultaneously (Korripally et al., 2015). On the contrary, the species that degrade lignin prior to polysaccharides are called selective lignin degraders, and include e.g. *Obba rivulosa* and *Gelatoporia* (*Ceriporiopsis*) *subvermispora* (Akhtar et al., 1997; Gupta et al., 2011; Hakala et al., 2004). These species are especially interesting in the biotechnological applications aiming to remove lignin (Hakala et al., 2004; Maijala et al., 2008).

O. rivulosa, a member of the *Gelatoporia* clade, is relatively common in North America (Nakasone, 1981), but sparsely distributed in Africa (Hjortstam and Ryvarden, 1996), Asia (Núñez and Ryvarden, 2001) and Europe (Ryvarden and Gilbertson, 1994), where it has been mostly isolated from coniferous softwood (Hakala et al., 2004). A dikaryotic *O. rivulosa* strain T241i (FBCC949) has been shown to degrade spruce softwood selectively (Hakala et al., 2004). Moreover, the *O. rivulosa* genome encodes a full set of lignocellulose-degrading genes, making it an interesting candidate for plant biomass research (Miettinen et al., 2016). Except for two MnPs and two laccases (Hakala et al., 2005; Hildén et al., 2013), no other lignocellulosic enzymes produced by *O. rivulosa* have been characterized, and therefore its mechanisms for plant cell wall degradation remain largely unknown.

Here we report temporal transcriptome analysis of *O. rivulosa* grown on its natural substrate, spruce wood. We used the genome-sequenced monokaryotic strain 3A-2, derived from the dikaryotic strain T241i, which has been previously studied in terms of selective lignin degradation. The expression of

genes encoding putative plant cell wall degrading CAZymes was studied after 2, 4 and 8 weeks of solid state cultivation in order to follow wood depolymerization in more natural like conditions. In addition, central carbon metabolic enzymes and fungal cell acting CAZymes encoding genes were studied to get insights into the nutritional demands during a prolonged cultivation on wood.

2. Materials and methods

2.1 Fungal strain and culture conditions

O. rivulosa monokaryon 3A-2 (FBCC1032) derived from the dikaryotic *O. rivulosa* strain T241i (FBCC949) was obtained from the HAMBI Fungal Biotechnology Culture Collection, University of Helsinki, Helsinki, Finland (fbcc@helsinki.fi). The fungus was maintained on 2% malt extract agar plates (MEA) (2% (w/v) malt extract, 2% (w/v) agar agar). For pre-cultures, the fungus was cultivated for 7 days at 28°C in 100 ml liquid low-nitrogen-asparagine-succinate medium (LN-AS), pH 4.5 (Hatakka and Uusi-Rauva, 1983), supplemented with 0.05% glycerol, in 250 ml Erlenmeyer flasks, which were inoculated with five mycelium-covered agar plugs (⌀ 7 mm) from MEA plates. After the homogenization (Waring Blender, USA), 4 ml of mycelial suspension was used for the inoculation of spruce wood solid cultures, which consisted of 2 g (dry weight) of Norway spruce (*Picea abies*) wood sticks (approx. 2 x 0.2 x 0.3 cm in size) on 1% (w/v) water agar (Mäkelä et al., 2002). Cultures were incubated stationary at 28°C in the dark for 2, 4, and 8 weeks. Three replicate control cultures inoculated with 4 ml of LN-AS supplemented with 0.05% glycerol were incubated similarly. After reaching the specific time point, mycelium-colonized wood sticks were flash frozen in liquid nitrogen followed by subsequent RNA extraction.

2.2 RNA extraction, cDNA library preparation and RNA sequencing

Total RNA was extracted from the spruce cultures by using a CsCl gradient ultracentrifugation as described previously (Patyshakuliyeva et al., 2014). Quality and quantity of RNA were determined by using the RNA6000 Nano Assay (Agilent 2100 Bioanalyzer, Agilent Technologies, Santa Clara, CA, USA). Purification of mRNA, synthesis of cDNA library, and sequencing (RNA-seq) was performed at the BGI Tech Solutions Co. Ltd. (Hong Kong, China) as described in Patyshakuliyeva et al. (2015). On average, 51 bp sequenced reads were constituted, producing approximately 557 MB raw yields for each sample. RNA-seq data was analyzed and statistically treated as described previously (Patyshakuliyeva et al., 2015). Raw reads were produced by base calling from the original image data. After that, data filtering was performed. Adaptor sequences, reads with unknown bases (N) >10% and low quality reads (more than 50% of the bases with quality values<5%) were removed. Clean reads were mapped to the genome sequence of *O. rivulosa* 3A-2 (v1.0 annotation, http://genome.jgi.doe.gov/Obbri1, (Miettinen et al., 2016)) using BWA/Bowtie (Langmead et al., 2009; Li and Durbin, 2010). On average, 82% total mapped read to the gene was achieved. The expression level was calculated as Fragments Per Kilobase of exon model per Million fragments mapped (FPKM) by using RSEM tool (Li and Dewey, 2011). Genes with FPKM value <20 under all conditions were considered as not expressed and filtered out of the analysis, and genes showing FPKM value ≥20 were considered as significantly expressed. Genes with FPKM value from 20 to 100 were considered as lowly, 100 to 300 as moderately and over 300 as highly expressed (approximately top 10% of the genes). Differential expression was identified by Student's T-test. A cut-off of fold change of >1.5 and P-value of <0.05 were used to identify differentially expressed genes between the time points. Genome-wide principal component analysis (PCA) of the gene expression on duplicate samples of the three time points was generated using FactoMineR package from Rcomander v.2.1-7 program in R statistical language and environment 3.1.2. (Lê et al., 2008). The RNA-seq data have been submitted to Gene Expression Omnibus (GEO) (Edgar et al., 2001) with GEO ID: GSE99871.

156

157 *2.3 Validation of RNA-seq expression patterns by qRT-PCR*

158 Smart RACE cDNA Amplification Kit (Clontech) was used for the cDNA synthesis according to the
159 manufacturer's instructions. 1 µg of RNA originating from two replicate cultures of *O. rivulosa* that
160 were used in RNA-seq was converted to cDNA in 20 µL reaction with Smart RACE cDNA
161 Amplification Kit (Clontech) and SuperScript III reverse transcriptase (Invitrogen) according to the
162 instructions of the manufacturers.

163

164 The relative amounts of nine selected gene transcripts were determined by qRT-PCR analysis to
165 validate the RNA-seq expression patterns. Gene-specific primers spanning exon-exon junction
166 (Supplementary Table 1) were designed according to the genome of *O. rivulosa* 3A-2
167 (http://genome.jgi.doe.gov/Obbri1, Miettinen et al., 2016) with PerlPrimer software (Marshall, 2004).
168 The amplification efficiency (E) of the primers was calculated from the slope of standard curve made
169 with template cDNA serial dilutions using the formula: $E= [10^{(-1/slope)} -1] \times 100$. The E-values of the
170 primer pairs varied from 94% to 102%, whereas, the R^2 values, ranged from 0.993 to 0.999
171 (Supplementary Table 1).

172

173 Three technical replicate qRT-PCR reactions were conducted for each sample and primer pair using
174 CFX96 Real-Time System C1000 Touch Thermal Cycler (Bio-Rad, USA). The 20 µL reactions
175 comprised of 30 ng cDNA template, 0,4 µM forward and reverse primer, 1 X DyNAmo HS SYBR
176 Green qPCR master mix (Thermo Scientific), and H_2O to the final volume of 20 µL. Cycling protocol
177 was: initial denaturation at 95°C followed by 35 cycles of (1) denaturation at 94°C for 10 s, (2)
178 annealing at 56°C for 20 s, and (3) extension at 72°C for 30 s. Fluorescence data acquisition was done
179 during the extension step. To confirm the specificity of the qRT-PCR primers, melting curve was

generated and inspected for the presence of a single peak. Relative expression levels were calculated by $2^{-\Delta\Delta Ct}$ method (Livak and Schmittgen, 2001) for the *gapdh*-normalized cycle threshold (Ct) values and the results are reported as relative fold changes.

3. Results

The monokaryotic *O. rivulosa* 3A-2 strain grown on solid spruce wood was subjected to the time-scale transcriptomics study to compare the gene expression at different growth stages of the fungus. PCA analysis showed that the duplicate RNA samples used for RNA-seq were highly reproducible (Supplementary Fig. 1). In addition, the expression patterns obtained by RNA-seq analysis corresponded well to the qRT-PCR results of the nine selected putative CAZyme-encoding genes (Fig. 1). Similar to other Polyporales species, the genome of *O. rivulosa* contains a full repertoire of putative CAZyme-encoding genes targeted to plant cell wall degradation (Miettinen et al., 2016). In total, 259 different putative CAZyme-encoding genes were significantly expressed in *O. rivulosa* cultures, and of these 110 were predicted to encode plant cell wall degrading enzymes (PCWDEs) (Fig. 2A) from 35 different CAZy families (Supplementary Table 2). Transcripts encoding putative GHs were the most abundant ones with 138 detected transcripts (53% of total PCWDE CAZys). The CAZymes-encoding transcripts from AAs, GTs, CEs, and PLs represented 15%, 30%, 7%, and 2.5% of the total PCWDE CAZy transcripts detected, respectively. Of these, 20, 31, and 16 CAZy genes are putatively targeted towards cellulose, hemicellulose and lignin, respectively (Fig. 2A). 16 genes encoding putatively H_2O_2-supplying enzymes were detected, while 6 and 5 genes encoding pectin and starch depolymerizing enzymes were expressed, respectively. Diverse activities included 16 CAZy transcripts, which can have activity towards multiple substrates. Highly expressed PCWDE CAZyme encoding transcripts belonged to 20 different CAZy families with varying gene numbers (Fig. 2B). All genes from cellulose

acting GH6, GH12 and AA8-A3_1, xyloglucan acting GH73 and pectin acting GH53 and GH88 families showed high expression (Fig. 2B).

As a typical white-rot fungal species, *O. rivulosa* harbors multiple genes predicted to be involved in lignin degradation in its genome. Of these, two putative MnP (Protein IDs 806545 and 835392) encoding genes were the highest expressed PCWDE CAZy transcripts during the cultivation. Interestingly, they showed unusually high expression levels throughout the cultivation peaking from 20 000 to 22 000 FPKM after 4-week cultivation (Table 1). This may suggest an important role for the corresponding enzymes in lignin degradation during the growth of *O. rivulosa* monokaryon on spruce. Three putative AA1_1 laccases were also detected on spruce, but none of those was highly expressed (Supplementary Table 3A). In addition to the laccases, *O. rivulosa* multicopper oxidase-encoding transcripts included one AA1_2 ferroxidase (FET), which compared to the laccases was moderately expressed. Production of hydrogen peroxide is essential for the lignin degradation since it is a prerequisite for peroxidase activity. In accordance with that, 10 transcripts predicted to encode family AA3_2 and AA3_3 glucose methanol choline (GMC) oxidoreductases were detected. Although most of the transcripts encoding the putative GMCs showed low expression, interestingly, one of the transcripts encoding an AA3_3 alcohol oxidase (AOX; 790443) was highly expressed in all time points, and was the most abundant transcript among lignin degradation-related transcripts after two AA2 MnPs. These findings confirm the major importance of peroxidases and hydrogen peroxide-producing machinery for the lignocellulose conversion in *O. rivulosa*.

Of the transcripts predicted to encode cellulolytic activities, β-1,4-endoglucanases (EGLs), cellobiohydrolases (CBHs), β-1,4-glucosidases (BGLs) and LPMOs were the most abundant ones among all the growth stages of *O. rivulosa* on wood (Supplementary Fig. 2, Supplementary Table 3A).

In total, 9 transcripts encoding putative EGLs from GH5, 12, 45 and 131 were detected. Six of those were highly expressed after 2 weeks with a 98- to 17- fold downregulation at the later stages (Supplementary Table 3A). The *O. rivulosa* genome possesses one GH6 cellobiohydrolase II (CBHII) and two GH7 CBHIs, of which the CBHII (Protein ID 476379) as well as one CBHI (Protein ID 731121) were highly expressed after 2 weeks. Interestingly, their expression decreased to moderate and low levels after 4 and 8 weeks of cultivation, respectively. A third important hydrolytic cellulose-acting enzymes are encoded by the enzyme families GH1 and GH3. Although seven BGL encoding genes were present in the transcriptome, only one GH3 BGL (Protein ID 14692) was highly expressed after 2-week cultivation. Genes encoding seven putative LPMOs oxidatively cleaving plant cell wall polysaccharides were also expressed (Supplementary Table 3A). Of these, six were found to be highly expressed, most of them after 2 weeks of cultivation. Interestingly, one LPMO (Protein ID 794851) encoding gene was highly expressed throughout the cultivation.

The most abundant transcript predicted to act on hemicellulose was a GH5 mannanase (MAN; Protein ID 641261), which was the third most abundant transcript in general (Table 1). Overall, three transcripts predicted to encode GH5 MANs were detected. Among four detected GH27 α-galactosidases (AGLs), only one was highly expressed (Protein ID 849432). Six genes encoding GH10 endoxylanases, 4 of which were highly expressed at the early cultivation stage (Protein IDs 838746, 851185, 762583 and 799009), were detected in the cultures. In addition, genes encoding one putative α-glucuronidase (AGU; Protein ID 726547) and one putative xyloglucanase (XG-EG; Protein ID 808997) showed high expression levels. Interestingly, almost all predicted hemicellulose degrading enzyme encoding genes showed higher abundances in early stages of wood decay with subsequent decrease. Only one GH2 mannosidase (MND; Protein ID 753990) was expressed at a constant, moderate level at

all three time points. High expression was not detected for any of the putative hemicellulases encoding genes after 4 or 8 weeks of cultivation.

In addition to the hemicellulose specific GHs, differential abundances of transcripts predicted to encode one hemicellulose acting glucuronoyl esterase (GE; Protein ID 762191) and three multiple substrates acting acetyl esterases (AE; Protein IDs 749512, 724015 and 816606) from carbohydrate esterase (CE) families 15 and 16, respectively, were detected. Similar to hemicellulose degrading GH families, their expression trend showed the highest transcript abundances in early cultivation stage.

Overall, the expression of the PCWDE CAZy genes was highest after 2-week growth of *O. rivulosa* and reduced markedly over time (Supplementary Table 3A, Supplementary Fig. 2). The only exceptions were MnPs, LCCs, AAOs and a single copy of PGA and GAL. When the sum of the transcript levels per putative CAZy enzyme activity was compared during the cultivation, MnPs were the most highly expressed, followed by LPMOs, XLNs, CBHs and MANs, respectively (Supplementary Fig. 2).

Altogether 22% (13 out of 60) of predicted fungal cell wall encoding CAZymes were highly expressed in all three time points (Supplementary Table 3B). These genes showed an interesting trend of either being highly expressed throughout the cultivation or showing high level expression at the early stage with a decreasing trend after 4-week cultivation, followed by an upregulation at the last time point after 8 weeks (Supplementary Table 3B). This could suggest possible recycling of fungal cell wall polysaccharides by *O. rivulosa*, such as α-1,3-, β-1,3- and β-1,6-glucans, which can be hydrolyzed to glucose and reutilized by the fungus. The overall highest transcript abundancy was detected for one gene encoding a putative GH131 β-glucanase (Protein ID 812963), acting on β-(1,3)-/β-(1,6)- and β-

(1,4)-linked glucan substrates, after 2-week cultivation. Other highly expressed genes in the early time point were two GH16 β-1,3(4)-endoglucanases, a GH18 chitinase and GH55 β-1,3-endoglucanase. Constantly highly expressed transcripts included a CE4 chitin deacetylase, a GH16 β-1,3(4)-endoglucanase, two β-1,3-endoglucanases from GH16 and GH128, a GH16 licheninase and a GH18 chitinase.

Despite the downregulated expression of the genes encoding CAZymes targeted for carbon acquisition from plant biomass, *O. rivulosa* showed active mycelial growth throughout the cultivation (Fig. 3). This was also confirmed by the expression of the carbon metabolic genes showing that all central carbon metabolic pathways were active in all studied time points. This suggests that *O. rivulosa* was not under carbon starvation during the cultivation (Supplementary Table 3C, Supplementary Fig. 3). D-glucose, D-mannose and D-xylose are the major monosaccharides originating from spruce wood polysaccharides, while smaller amounts of D-galactose, L-arabinose and L-rhamnose are also present (Rytioja et al., 2017). Hexose monomers can be converted through glycolysis, which is connected to pentose phosphate pathway (PPP). Among the glycolysis genes, *pki1*, encoding pyruvate kinase, catalyzing the last step of the glycolysis, as well as genes encoding glucose-6-phosphate isomerase (*pgi1*), fructose-2,6-bisphosphatase (*pfk2*), fructose-bisphosphate aldolase (*fba1*), glyceraldehyde-3-phosphate dehydrogenase (*gpd1*), and enolase (*eno1*), showed high expression (Supplementary Fig. 3A). While *pgi1*, *pfk2* and *fba1* showed decreasing expression during the cultivation, *gpd1* and *eno1* were upregulated. Isocitrate lyase (*icl1*), malate dehydrogenase (*mdh1*) and related oxaloacetase (*oxa1*) encoding genes involved in the tricarboxylic acid (TCA) cycle were highly expressed (Supplementary Fig. 3A). A gene encoding 6-phosphogluconate dehydrogenase (*gnd1*) as well as one of the transaldolases encoding genes (*tal2*) of the PPP showed constant high level expression throughout the cultivation (Supplementary Fig. 3B). Pentoses D-xylose and L-arabinose originating from

hemicelluloses and pectin are catabolized through the pentose catabolic pathway (PCP). High level expression was detected for two out of the three PCP genes identified in *O. rivulosa*, i.e. L-arabinose reductase (*lar1*) and xylitol dehydrogenase (*xdh1*) (Supplementary Fig. 3B). However, all three PCP genes were downregulated after 2-week growth. It should be noted that we were not able to identify (based on similarity to known ascomycete genes) some of the carbon metabolic genes in *O. rivulosa*, including half of the genes encoding PCP enzymes (Supplementary Fig. 3). The pathways for catabolism of pectin-derived L-rhamnose and D-galacturonic acid, as well as the Leloir pathway for D-galactose present in hemicelluloses and pectin were also active (Supplementary Fig. 3C).

4. Discussion

In this work, we studied the transcriptomic response of the white-rot fungus *O. rivulosa* during a prolonged cultivation period of 8 weeks on solid spruce to evaluate changes in gene expression during the lengthy process of fungal wood colonization. The genome-sequenced monokaryotic *O. rivulosa* strain 3A-2 (Miettinen et al., 2016) was used, and the focus was on the analysis of the genes encoding plant cell wall polymers degrading CAZymes that are responsible for carbon acquisition from plant biomass. Also, carbon metabolic genes and fungal cell wall degrading enzymes were evaluated to get a collective overview of ongoing metabolic processes.

Our results show that *O. rivulosa* highly expresses the genes encoding a complete repertoire of enzymes for degradation of cellulose, hemicellulose and lignin on spruce, similarly to other white rot species including *Dichomitus squalens* (Rytioja et al., 2017) and *Phlebia radiata* (Kuuskeri et al., 2016). Interestingly, almost all of the detected plant cell wall acting CAZy genes were highly expressed after 2-week growth of *O. rivulosa*, while most of them were strongly downregulated in the later time points. Generally regarded as key enzymes of white rot fungal ligninolytic system, class II heme

peroxidases are abundantly represented in the genome of *O. rivulosa*, including 11 MnPs, and one LiP from family AA2 (Miettinen et al., 2016). Among nine putative MnP encoding transcripts detected in spruce cultivations, five genes were highly expressed of which two (Protein IDs 806545 and 835392) exhibited unusually high FPKM levels throughout the cultivation and had the highest transcript abundances at 4-week time point. MnPs have often been shown to be constantly produced by white-rot fungi throughout the solid state cultivation on wood (Aguiar et al., 2006; Galliano et al., 1991; Hakala et al., 2005), which is in line with the high expression of the two putative MnP transcripts of *O. rivulosa*.

Expression levels of the LiP encoding gene were negligible (FPKM<20) suggesting only minor input in lignin degradation by *O. rivulosa*. This is in accordance with the results from *G. subvermispora*, a close relative of *O. rivulosa*, where a putative LiP was not upregulated in aspen cultures compared to glucose medium (Fernandez-Fueyo et al., 2012). On the contrary, the non-selective white-rot fungi, such as *P. chrysosporium* (Vanden Wymelenberg et al., 2010), *Phanerochaete carnosa* (MacDonald et al., 2011) and *P. radiata* (Kuuskeri et al., 2016), have shown significant upregulation of several LiP encoding genes on wood substrates, implying differences in lignin degradation approaches between the white-rot fungal species.

Three out of nine putative AA1_1 laccase genes of *O. rivulosa* were expressed on spruce, but none of those was highly expressed. This is in contrast with *G. subvermispora* (Fernandez-Fueyo et al., 2012) and *D. squalens* (Rytioja et al., 2017) laccases, which were significantly upregulated in the agitated liquid cultures supplemented with milled aspen wood and spruce sawdust, respectively. However, our finding was consistent with that from the solid spruce cultures of the white-rot fungus *P. radiata*, showing low expression of laccase-encoding genes after 4-weeks of cultivation (Kuuskeri et al., 2016).

346 This may indicate that in the shaken liquid cultures, laccases defend the fungal mycelium against
347 oxidative stress (Jaszek et al., 2006; Joo et al., 2008), whereas in the more natural like solid state
348 cultivations, their role in lignin degradation is controversial. Nevertheless, acidic laccase isoforms have
349 been purified from the early phase of the solid spruce chip cultures of *O. rivulosa* despite of the minor
350 laccase activity detected from the cultivations (Hakala et al., 2005). This could indicate that laccases
351 may have a role in initial wood colonization.
352
353 The dikaryotic *O. rivulosa* strain T241i has been shown to selectively degrade spruce by decomposing
354 lignin prior to cellulose (Hakala et al., 2004). However, the results of our study do not indicate
355 selective lignin degradation by the monokaryotic *O. rivulosa* 3A-2, as genes encoding enzymes
356 targeted towards all plant biomass polymers were simultaneously highly expressed. A high level of
357 diversity within the white rot fungal species has often been reported. These include discrepancies
358 regarding enzyme production profile and lignin degrading ability between *Pleurotus osteratus*
359 monokaryon and its parental dikaryon. In solid state fermentation, the monokaryon showed higher
360 lignin-modifying enzyme activities, but a lower rate of lignin degradation compared to the dikaryon
361 (Eichlerová et al., 2000). Highly variable lignocellulose acting enzyme profiles have also been detected
362 between the mono- and dikaryotic strains of *D. squalens* (Casado-López et al., 2017). In addition,
363 higher levels of ligninolytic enzyme activities have been produced by monokaryotic strains of the
364 white-rot fungi *Pycnopours cinnabarinus* (Herpoël et al., 2000), *Pycnoporus sanguineus* (Lomascolo et
365 al., 2002), *P. ostreatus* (Eichlerová et al., 2002) and *Trametes hirsuta* (Li et al., 2012) compared to the
366 parental dikaryon.
367
368 Selective lignin degradation seems also to be temporally regulated, as the selectivity is usually limited
369 to early stages of decay (Adaskaveg et al., 1995; Ferraz et al., 2000). It may be possible that the 2-week

time point was too late to detect the initial lignin degradation selectivity at the transcript level in the *O. rivulosa* 3A-2 cultures, although its parental dikaryon T241i has maintained the selectivity during prolonged cultivation (Hakala et al., 2004). Selectivity of white-rot wood degradation is also dependent on the physical and chemical parameters, such as temperature, and oxygen and moisture content, in wood (Adaskaveg et al., 1995; Blanchette, 1995). *O. rivulosa* T241i has been shown to degrade lignin selectively when grown on spruce wood blocks at 25°C (Hakala et al. 2004), thus differing slightly from the conditions used in this study for *O. rivulosa* 3A-2.

In addition to plant polymers degrading enzymes of *O. rivulosa* assessed in this study, we also evaluated enzymes involved in the major carbon metabolic pathways. Carbon catabolic genes were expressed throughout the 8-week cultivation demonstrating good metabolic activity of the fungus during lengthy wood colonization and conversion in laboratory conditions. Overall, higher expression was detected for genes encoding enzymes involved in glycolysis and PPP than for those involved in PCP. A similar trend has been reported from the compost grown litter decomposing *Agaricus bisporus* (Patyshakuliyeva et al., 2015), possibly suggesting a preferred use of hexoses over pentoses. Among TCA and glyoxalate cycle related genes, malate dehydrogenase (*mdh1*) and oxaloacetase (*oxa1*) showed the highest transcript levels during growth of *O. rivulosa* on spruce. Oxalate synthesis has been suggested to be coupled with energy production in brown-rot fungi *Fomitopsis palustris* (Munir et al., 2001) and *Postia placenta* (Martinez et al., 2009) by Mdh1, which generates energy by oxidizing malate to oxaloacetate, which is then converted to oxalate by Oxa1. In addition, a number of roles for oxalate with respect to lignocellulose degradation has been proposed, including acidification of fungal extracellular environment to the levels that are usually needed for the activity of lignin acting enzymes (Mäkelä et al., 2010). *O. rivulosa* has been shown to produce oxalate during growth on spruce wood

chips (Hakala et al., 2005), which is in line with the constant high expression of *oxa1* in *O. rivulosa* observed in our study.

Fungal cell wall acting enzymes comprising mostly chitinases and various β-glucanases are important for cell wall remodeling during active hyphal growth, as well as aging-related cell wall recycling (Gruber and Seidl-Seiboth, 2012). The most numerous representatives of the genes encoding putative fungal cell wall acting enzymes expressed by *O. rivulosa* were family GH16 members that are involved in chitin-β-1,3-glucan formation, suggesting a role in the processing of the fungal cell wall polysaccharides (Klis et al., 2007). Two out of 11 putative GH18 chitinases encoding genes of *O. rivulosa* showed constant high-level expression suggesting continuous recycling of chitin during the cultivation. In ectomycorrhizal fungus *Laccaria bicolor* GH18 chitinase genes are also found to be upregulated in free-living mycelium implying possible degradation of exogenous fungal cell wall (Veneault-Fourrey et al., 2014).

Our results suggest that during the growth of *O. rivulosa* monokaryon 3A-2 on its natural substrate, spruce wood, the highest expression of genes involved in plant cell wall degradation occurs at early stages of wood colonization. The simultaneous expression of genes targeted towards all lignocellulosic polymers suggests that *O. rivulosa* 3A-2 does not selectively remove spruce wood lignin. Thus, these results indicate high variation within mono- and dikaryotic strains of white-rot fungal species towards lignocellulose degradation.

Acknowledgements

MM was supported by the Academy of Finland research grant no: 297847 and the European Commission, Marie Curie ITN network Subicat FP7 Grant agreement no: 607044, and OM by Marie Curie fellowships PIOF-GA-2011-302349. MVA-P was supported by a grant of the Dutch Technology Foundation STW, Applied Science division of NWO, and the Technology Program of the Ministry of Economic Affairs 016.130.609 to RPdV.

References

Adaskaveg, J.E., Gilbertson, R.L., Dunlap, M.R., 1995. Effects of incubation time and temperature on in vitro selective delignification of silver leaf oak by *Ganoderma colossum*. Appl. Environ. Microbiol. 61, 138-144.

Aguiar, A., de Souza-Cruz, P.B., Ferraz, A., 2006. Oxalic acid, Fe^{3+}-reduction activity and oxidative enzymes detected in culture extracts recovered from *Pinus taeda* wood chips biotreated by *Ceriporiopsis subvermispora*. Enzyme Microb. Technol. 38, 873-878.

Akhtar, M., Blanchette, R.A., Kirk, T.K., 1997. Fungal delignification and biomechanical pulping of wood. In: Eriksson, K.-E.L. (Ed.), Biotechnology in the Pulp and Paper Industry. Springer Berlin Heidelberg, Berlin, Heidelberg, pp. 159-195.

Blanchette, R.A., 1995. Degradation of the lignocellulose complex in wood. Can. J. Bot. 73, 999-1010.

Cantarel, B.L., Coutinho, P.M., Rancurel, C., Bernard, T., Lombard, V., Henrissat, B., 2008. The Carbohydrate-Active EnZymes database (CAZy): an expert resource for glycogenomics. Nucleic Acids Res. 37, D233-238.

Casado-López, S., Theelen, B., Manserra, S., Issak, T.Y., Rytioja, J.T., Mäkelä, M.R., de Vries, R., 2017. Functional diversity in *Dichomitus squalens* monokaryons. IMA Fungus 8, 17-25.

Edgar, R., Domrachev, M., Lash, A.E., 2001. Gene Expression Omnibus: NCBI gene expression and hybridization array data repository. Nucleic Acids Res. 30, 207-210.

Eichlerová, I., Homolka, L., Nerud, F., 2002. Decolorization of synthetic dyes by *Pleurotus ostreatus* isolates differing in ligninolytic properties. Folia Microbiol. 47, 691-695.

Eichlerová, I., Ruel, K., Homolka, L., Joseleau, J.P., Nerud, F., 2000. Ligninolytic characteristics of *Pleurotus ostreatus* strain F6 and its monokaryotic protoplast derivative P19. Can. J. Microbiol. 46, 1153-1158.

Fernandez-Fueyo, E., Ruiz-Dueñas, F.J., Ferreira, P., Floudas, D., Hibbett, D.S., Canessa, P., Larrondo, L.F., James, T.Y., Seelenfreund, D., Lobos, S., Polanco, R., Tello, M., Honda, Y., Watanabe, T., Watanabe, T., Ryu, J.S., Kubicek, C.P., Schmoll, M., Gaskell, J., Hammel, K.E., St. John, F.J., Vanden Wymelenberg, A., Sabat, G., Splinter BonDurant, S., Syed, K., Yadav, J.S., Doddapaneni, H., Subramanian, V., Lavín, J.L., Oguiza, J.A., Perez, G., Pisabarro, A.G., Ramirez, L., Santoyo, F., Master, E., Coutinho, P.M., Henrissat, B., Lombard, V., Magnuson, J.K., Kües, U., Hori, C., Igarashi, K., Samejima, M., Held, B.W., Barry, K.W., LaButti, K.M., Lapidus, A., Lindquist, E.A., Lucas, S.M., Riley, R., Salamov, A.A., Hoffmeister, D., Schwenk, D., Hadar, Y., Yarden, O., de Vries, R.P., Wiebenga, A., Stenlid, J., Eastwood, D., Grigoriev, I.V., Berka, R.M., Blanchette, R.A., Kersten, P., Martinez, A.T., Vicuna, R., Cullen, D., 2012. Comparative genomics of *Ceriporiopsis subvermispora* and *Phanerochaete chrysosporium* provide insight into selective ligninolysis. Proc. Natl. Acad. Sci. U. S. A. 109, 5458-5463.

Ferraz, A., Parra, C., Freer, J., Baeza, J., Rodríguez, J., 2000. Characterization of white zones produced on *Pinus radiata* wood chips by *Ganoderma australe* and *Ceriporiopsis subvermispora*. World J. Microbiol. Biotechnol. 16, 641-645.

Ferreira, P., Carro, J., Serrano, A., Martínez, A.T., 2015. A survey of genes encoding H_2O_2-producing GMC oxidoreductases in 10 Polyporales genomes. Mycologia 107, 1105-1119.

Galliano, H., Gas, G., Seris, J.L., Boudet, A.M., 1991. Lignin degradation by *Rigidoporus lignosus* involves synergistic action of two oxidizing enzymes: Mn peroxidase and laccase. Enzyme Microb. Technol. 13, 478-482.

Gruber, S., Seidl-Seiboth, V., 2012. Self versus non-self: fungal cell wall degradation in *Trichoderma*. Microbiology 158, 26-34.

Gupta, R., Mehta, G., Khasa, Y.P., Kuhad, R.C., 2011. Fungal delignification of lignocellulosic biomass improves the saccharification of cellulosics. Biodegradation 22, 797-804.

Hakala, T.K., Hildén, K., Maijala, P., Olsson, C., Hatakka, A., 2006. Differential regulation of manganese peroxidases and characterization of two variable MnP encoding genes in the white-rot fungus *Physisporinus rivulosus*. Appl. Microbiol. Biotechnol. 73, 839-849.

Hakala, T.K., Lundell, T., Galkin, S., Maijala, P., Kalkkinen, N., Hatakka, A., 2005. Manganese peroxidases, laccases and oxalic acid from the selective white-rot fungus *Physisporinus rivulosus* grown on spruce wood chips. Enzyme Microb. Technol. 36, 461-468.

Hakala, T.K., Maijala, P., Konn, J., Hatakka, A., 2004. Evaluation of novel wood-rotting polypores and corticioid fungi for the decay and biopulping of Norway spruce (*Picea abies*) wood. Enzyme Microb. Technol. 34, 255-263.

476 Hatakka, A., Hammel, K.E., 2011. Fungal biodegradation of lignocelluloses. In: Hofrichter, M. (Ed.),
477 Industrial Applications, The Mycota. Springer Berlin Heidelberg, Berlin, Heidelberg, pp. 319-340.

478 Hatakka, A.I., Uusi-Rauva, A., 1983. Degradation of ^{14}C-labelled poplar wood lignin by selected
479 white-rot fungi. Eur. J. Appl. Microb. Biotechnol. 17, 235-242.

480 Herpoël, I., Moukha, S., Lesage-Meessen, L., Sigoillot, J., Asther, M., 2000. Selection of *Pycnoporus*
481 *cinnabarinus* strains for laccase production. FEMS Microbiol. Lett. 183, 301-306.

482 Hildén, K., Mäkelä M.R., Lundell, T.K., Kuuskeri, J., Chernykh, A., Golovleva. L., Archer, D.B.,
483 Hatakka, A., 2007. Heterologous expression and structural characterization of two low pH laccases
484 from a biopulping white-rot fungus *Physisporinus rivulosus*. Appl. Microbiol. Biotechnol. 97, 1589-
485 1599.

486 Hjortstam, K., Ryvarden, L., 1996. New and interesting wood-inhabiting fungi (Basidiomycotina –
487 Aphyllophorales) from Ethiopia. Mycotaxon (LX) 60, 181-190.

488 Isikgor, F.H., Becer, C.R., 2015. Lignocellulosic biomass: a sustainable platform for the production of
489 bio-based chemicals and polymers. Polym. Chem. 6, 4497-4559.

490 Jaszek, M., Grzywnowicz, K., Malarczyk, E., Leonowicz, A., 2006. Enhanced extracellular laccase
491 activity as a part of the response system of white rot fungi: *Trametes versicolor* and *Abortiporus*
492 *biennis* to paraquat-caused oxidative stress conditions. Pestic. Biochem. Physiol. 85, 147-154.

493 Joo, S.S., Ryu, I.W., Park, J.K., Yoo, Y.M., Lee, D.H., Hwang, K.W., Choi, H.T., Lim, C.J., Lee, D.I.,
494 Kim, K., 2008. Molecular cloning and expression of a laccase from *Ganoderma lucidum*, and its
495 antioxidative properties. Mol. Cells 25, 112-118.

496 Khosravi, C., Benocci, T., Battaglia, E., Benoit, I., de Vries, R.P., 2015. Sugar catabolism in
497 *Aspergillus* and other fungi related to the utilization of plant biomass. Adv. Appl. Microbiol. 90, 1-28.

498 Klis, F.M., Ram, A.F.J., De Groot, P. W. J., 2007. A molecular and genomic view of the fungal cell
499 wall. In: Howard, R.J., Gow, N.A.R. (Eds.), Biology of the Fungal Cell. Springer Berlin Heidelberg,
500 Berlin, Heidelberg, pp. 97-120.

501 Korripally, P., Hunt, C.G., Houtman, C.J., Jones, D.C., Kitin, P.J., Cullen, D., Hammel, K.E., 2015.
502 Regulation of gene expression during the onset of ligninolytic oxidation by *Phanerochaete*
503 *chrysosporium* on spruce wood. Appl. Environ. Microbiol. 81, 7802-7812.

504 Kuuskeri, J., Häkkinen, M., Laine, P., Smolander, O., Tamene, F., Miettinen, S., Nousiainen, P.,
505 Kemell, M., Auvinen, P., Lundell, T., 2016. Time-scale dynamics of proteome and transcriptome of the
506 white-rot fungus *Phlebia radiata*: growth on spruce wood and decay effect on lignocellulose.
507 Biotechnol. Biofuels 9, 192.

508 Langmead, B., Trapnell, C., Pop, M., Salzberg, S.L., 2009. Ultrafast and memory-efficient alignment
509 of short DNA sequences to the human genome. Genome Biol. 10, R25.

510 Langston, J.A., Shaghasi, T., Abbate, E., Xu, F., Vlasenko, E., Sweeney, M.D., 2011. Oxidoreductive
511 cellulose depolymerization by the enzymes cellobiose dehydrogenase and glycoside hydrolase 61.
512 Appl. Environ. Microbiol. 77, 7007-7015.

513 Lê, S., Josse, J., Husson, F., 2008. FactoMineR: An R package for multivariate analysis. J. Stat.
514 Software 25, 1-18.

515 Li, B., Dewey, C.N., 2011. RSEM: accurate transcript quantification from RNA-Seq data with or
516 without a reference genome. BMC Bioinformatics 12, 323.

517 Li, H., Durbin, R., 2010. Fast and accurate long-read alignment with Burrows-Wheeler transform.
518 Bioinformatics 26, 589-595.

519 Li, J., Sun, F., Li, X., Yan, Z., Yuan, Y., Liu, X., 2012. Enhanced saccharification of corn straw
520 pretreated by alkali combining crude ligninolytic enzymes. J. Chem. Technol. Biotechnol. 87, 1687-
521 1693.

522 Livak, K.J., Schmittgen, T.D., 2001. Analysis of relative gene expression data using real-time
523 quantitative PCR and the $2^{-\Delta\Delta CT}$ method. Methods 25, 402-408.

524 Lomascolo, A., Cayol, J., Roche, M., Guo, L., Robert, J., Record, E., Lesage-Meessen, L., Ollivier, B.,
525 Sigoillot, J., Asther, M., 2002. Molecular clustering of *Pycnoporus* strains from various geographic
526 origins and isolation of monokaryotic strains for laccase hyperproduction. Mycol. Res. 106, 1193-1203.

527 Lombard, V., Golaconda Ramulu, H., Drula, E., Coutinho, P.M., Henrissat, B., 2013. The
528 carbohydrate-active enzymes database (CAZy) in 2013. Nucleic Acids Res. 42, D490-495.

529 MacDonald, J., Doering, M., Canam, T., Gong, Y., Guttman, D.S., Campbell, M.M., Master, E.R.,
530 2011. Transcriptomic responses of the softwood-degrading white-rot fungus *Phanerochaete carnosa*
531 during growth on coniferous and deciduous wood. Appl. Environ. Microbiol. 77, 3211-3218.

532 Maijala, P., Kleen, M., Westin, C., Poppius-Levlin, K., Herranen, K., Lehto, J.H., Reponen, P.,
533 Mäentausta, O., Mettälä, A., Hatakka, A., 2008. Biomechanical pulping of softwood with enzymes and
534 white-rot fungus *Physisporinus rivulosus*. Enzyme Microb. Technol. 43, 169-177.

535 Mäkelä, M., Galkin, S., Hatakka, A., Lundell, T., 2002. Production of organic acids and oxalate
536 decarboxylase in lignin-degrading white rot fungi. Enzyme Microb. Technol. 30, 542-549.

537 Mäkelä, M.R., Hildén, K.S., de Vries, R.P., 2014. Degradation and modification of plant biomass by
538 fungi. In: Nowrousian, M. (Ed.), Fungal Genomics. The Mycota. Springer Berlin Heidelberg, Berlin,
539 Heidelberg, pp. 175-208.

540 Mäkelä, M.R., Hildén, K., Lundell, T.K., 2010. Oxalate decarboxylase: biotechnological update and
541 prevalence of the enzyme in filamentous fungi. Appl. Microbiol. Biotechnol. 87, 801-814.

542 Marshall, O.J., 2004. PerlPrimer: cross-platform, graphical primer design for standard, bisulphite and
543 real-time PCR. Bioinformatics 20, 2471-2472.

544 Martinez, D., Challacombe, J., Morgenstern, I., Hibbett, D., Schmoll, M., Kubicek, C.P., Ferreira, P.,
545 Ruiz-Dueñas, F.J., Martinez, A.T., Kersten, P., Hammel, K.E., Vanden Wymelenberg, A., Gaskell, J.,
546 Lindquist, E., Sabat, G., Bondurant, S.S., Larrondo, L.F., Canessa, P., Vicuna, R., Yadav, J.,
547 Doddapaneni, H., Subramanian, V., Pisabarro, A.G., Lavin, J.L., Oguiza, J.A., Master, E., Henrissat,
548 B., Coutinho, P.M., Harris, P., Magnuson, J.K., Baker, S.E., Bruno, K., Kenealy, W., Hoegger, P.J.,
549 Kües, U., Ramaiya, P., Lucas, S., Salamov, A., Shapiro, H., Tu, H., Chee, C.L., Misra, M., Xie, G.,
550 Teter, S., Yaver, D., James, T., Mokrejs, M., Pospisek, M., Grigoriev, I.V., Brettin, T., Rokhsar, D.,
551 Berka, R., Cullen, D., 2009. Genome, transcriptome, and secretome analysis of wood decay fungus
552 *Postia placenta* supports unique mechanisms of lignocellulose conversion. Proc. Natl. Acad. Sci. U. S.
553 A. 106, 1954-1959.

554 Miettinen, O., Riley, R., Barry, K., Cullen, D., de Vries, R.,P., Hainaut, M., Hatakka, A., Henrissat, B.,
555 Hildén, K., Kuo, R., LaButti, K., Lipzen, A., Mäkelä, M.R., Sandor, L., Spatafora, J.W., Grigoriev,
556 I.V., Hibbett, D.S., 2016. Draft genome sequence of the white-rot fungus *Obba rivulosa* 3A-2. Genome
557 Announc. 4, e00976-16.

558 Munir, E., Yoon, J.J., Tokimatsu, T., Hattori, T., Shimada, M., 2001. A physiological role for oxalic
559 acid biosynthesis in the wood-rotting basidiomycete *Fomitopsis palustris*. Proc. Natl. Acad. Sci. U. S.
560 A. 98, 11126-11130.

561 Nakasone, K.K., 1981. Cultural studies on *Poria cinerascens*, *P. rivulosa*, and *P. subvermispora*
562 (Aphyllophorales, Basidiomycotina). Mycotaxon (XIII), 105-111.

563 Núñez, M., Ryvarden, L., 2001. East Asian polypores. Synopsis Fungorum 14, 170-522.

564 Patyshakuliyeva, A., Mäkelä, M.R., Sietiö, O.-M., de Vries, R.P., Hildén, K.S., 2014. An improved and
565 reproducible protocol for the extraction of high quality fungal RNA from plant biomass substrates.
566 Fungal Genet. Biol. 72, 201-206.

567 Patyshakuliyeva, A., Post, H., Zhou, M., Jurak, E., Heck, A.J.R., Hildén, K.S., Kabel, M.A., Mäkelä,
568 M.R., Altelaar, M.A.F., de Vries, R.P., 2015. Uncovering the abilities of *Agaricus bisporus* to degrade
569 plant biomass throughout its life cycle. Environ. Microbiol. 17, 3098-3109.

570 Rytioja, J., Hildén, K., Yuzon, J., Hatakka, A., de Vries, R.,P., Mäkelä, M.,R., 2014. Plant-
571 polysaccharide-degrading enzymes from basidiomycetes. Microbiol. Mol. Biol. Rev. 78, 614-649.

572 Rytioja, J., Hildén, K., Di Falco, M., Zhou, M., Aguilar-Pontes, M.V., Sietiö, O.-M., Tsang, A., de
573 Vries, R.P., Mäkelä, M.R., 2017. The molecular response of the white-rot fungus *Dichomitus squalens*
574 to wood and non-woody biomass as examined by transcriptome and exoproteome analyses. Environ.
575 Microbiol. 19, 1237-1250.

576 Ryvarden, L., Gilbertson, R.L., 1994. European polypores. Part 2. Synopsis Fungorum 7, 394-743.

Vaaje-Kolstad, G., Westereng, B., Horn, S.J., Liu, Z., Zhai, H., Sörlie, M., Eijsink, V.G.H., 2010. An oxidative enzyme boosting the enzymatic conversion of recalcitrant polysaccharides. Science 330, 219-222.

Vanden Wymelenberg, A., Gaskell, J., Mozuch, M., Sabat, G., Ralph, J., Skyba, O., Mansfield, S.D., Blanchette, R.A., Martinez, D., Grigoriev, I., Kersten, P.J., Cullen, D., 2010. Comparative transcriptome and secretome analysis of wood decay fungi *Postia placenta* and *Phanerochaete chrysosporium*. Appl. Environ. Microbiol. 76, 3599-3610.

Veneault-Fourrey, C., Commun, C., Kohler, A., Morin, E., Balestrini, R., Plett, J., Danchin, E., Coutinho, P., Wiebenga, A., de Vries, R.P., Henrissat, B., Martin, F., 2014. Genomic and transcriptomic analysis of *Laccaria bicolor* CAZome reveals insights into polysaccharides remodelling during symbiosis establishment. Fungal Genet. Biol. 72, 168-181.

Zhao, C., Xie, S., Pu, Y., Zhang, R., Huang, F., Ragauskas, A.J., Yuan, J.S., 2016. Synergistic enzymatic and microbial lignin conversion. Green Chem. 18, 1306-1312.

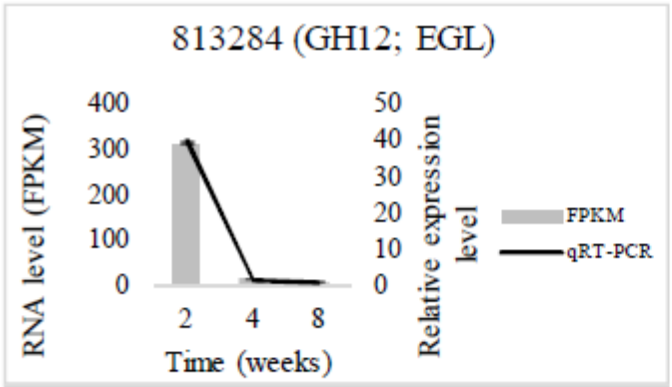
813284 (GH12; EGL)
RNA level (FPKM)
400
300
200
100
0
2
4
8
Time (weeks)
50
40
30
20
10
0
Relative expression level
FPKM
qRT-PCR

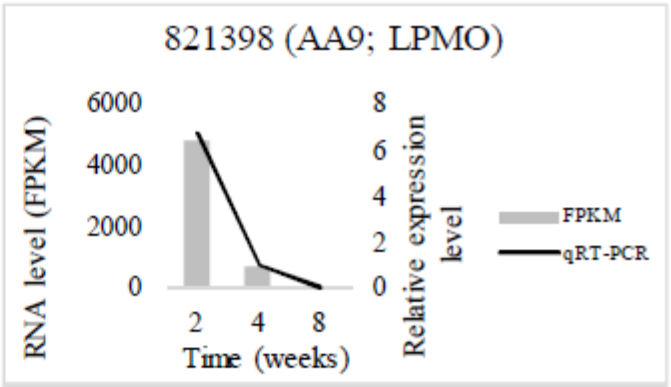
821398 (AA9; LPMO)
RNA level (FPKM)
6000
4000
2000
0
2
4
8
Time (weeks)
8
6
4
2
0
Relative expression level
FPKM
qRT-PCR

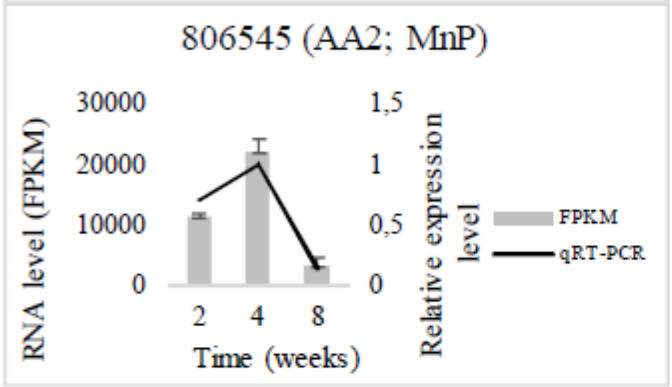
806545 (AA2; MnP)
RNA level (FPKM)
30000
20000
10000
0
2
4
8
Time (weeks)
1,5
1
0,5
0
Relative expression level
FPKM
qRT-PCR

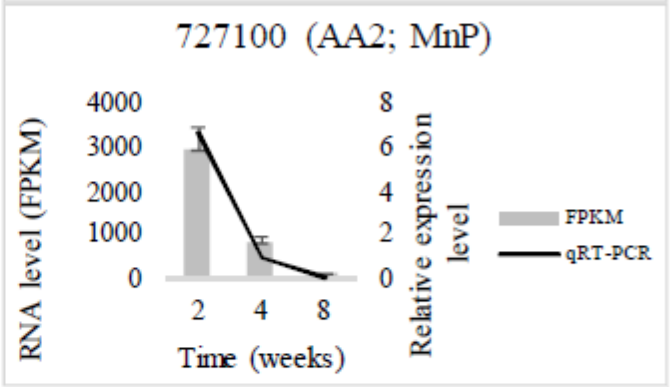
727100 (AA2; MnP)
RNA level (FPKM)
4000
3000
2000
1000
0
2
4
8
Time (weeks)
8
6
4
2
0
Relative expression level
FPKM
qRT-PCR

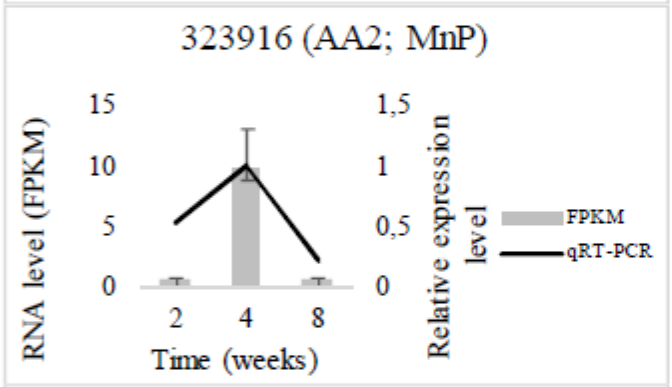
323916 (AA2; MnP)
RNA level (FPKM)
15
10
5
0
2
4
8
Time (weeks)
1,5
1
0,5
0
Relative expression level
FPKM
qRT-PCR

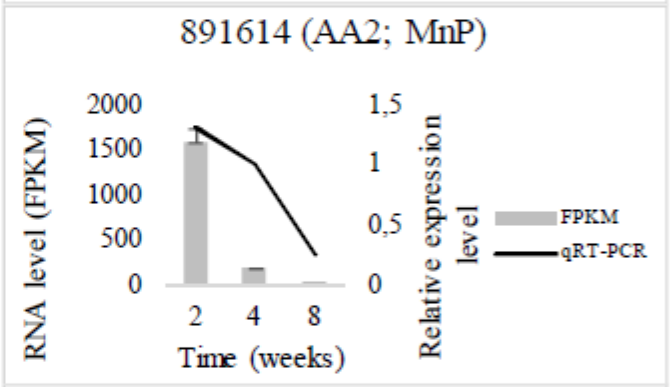
891614 (AA2; MnP)
RNA level (FPKM)
2000
1500
1000
500
0
2
4
8
Time (weeks)
1,5
1
0,5
0
Relative expression level
FPKM
qRT-PCR

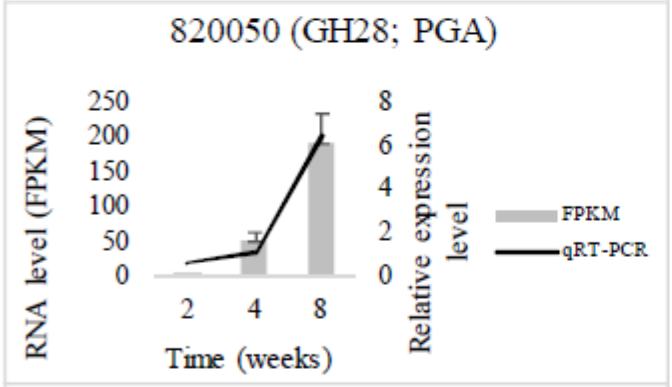
820050 (GH28; PGA)
RNA level (FPKM)
250
200
150
100
50
0
2
4
8
Time (weeks)
8
6
4
2
0
Relative expression level
FPKM
qRT-PCR

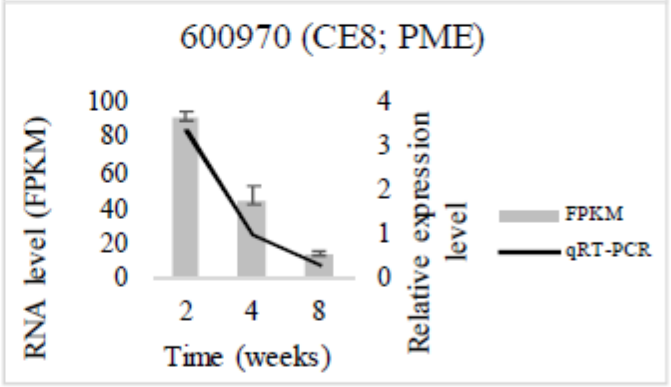
600970 (CE8; PME)
RNA level (FPKM)
100
80
60
40
20
0
2
4
8
Time (weeks)
4
3
2
1
0
Relative expression level
FPKM
qRT-PCR

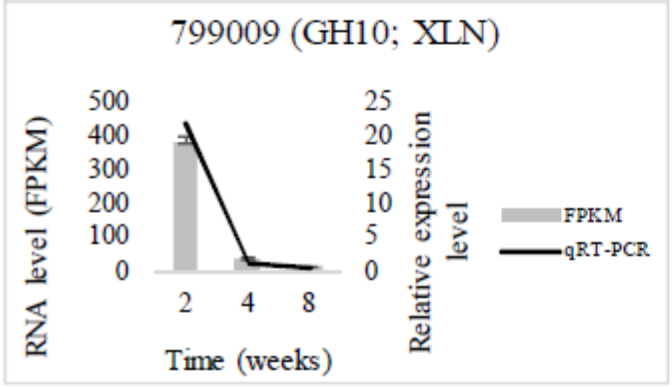
799009 (GH10; XLN)
RNA level (FPKM)
500
400
300
200
100
0
2
4
8
Time (weeks)
25
20
15
10
5
0
Relative expression level
FPKM
qRT-PCR

591

Figure 1. Validation of RNA-seq analysis by qRT-PCR of nine selected genes involved in plant cell wall degradation in *O. rivulosa*. Columns represent RNA level (FPKM), lines represent qRT-PCR values (relative unit). Error bars represent standard deviation of two biological replicates and three replicate qRT-PCR reactions. Enzyme abbreviations are presented in Supplementary Table 2.

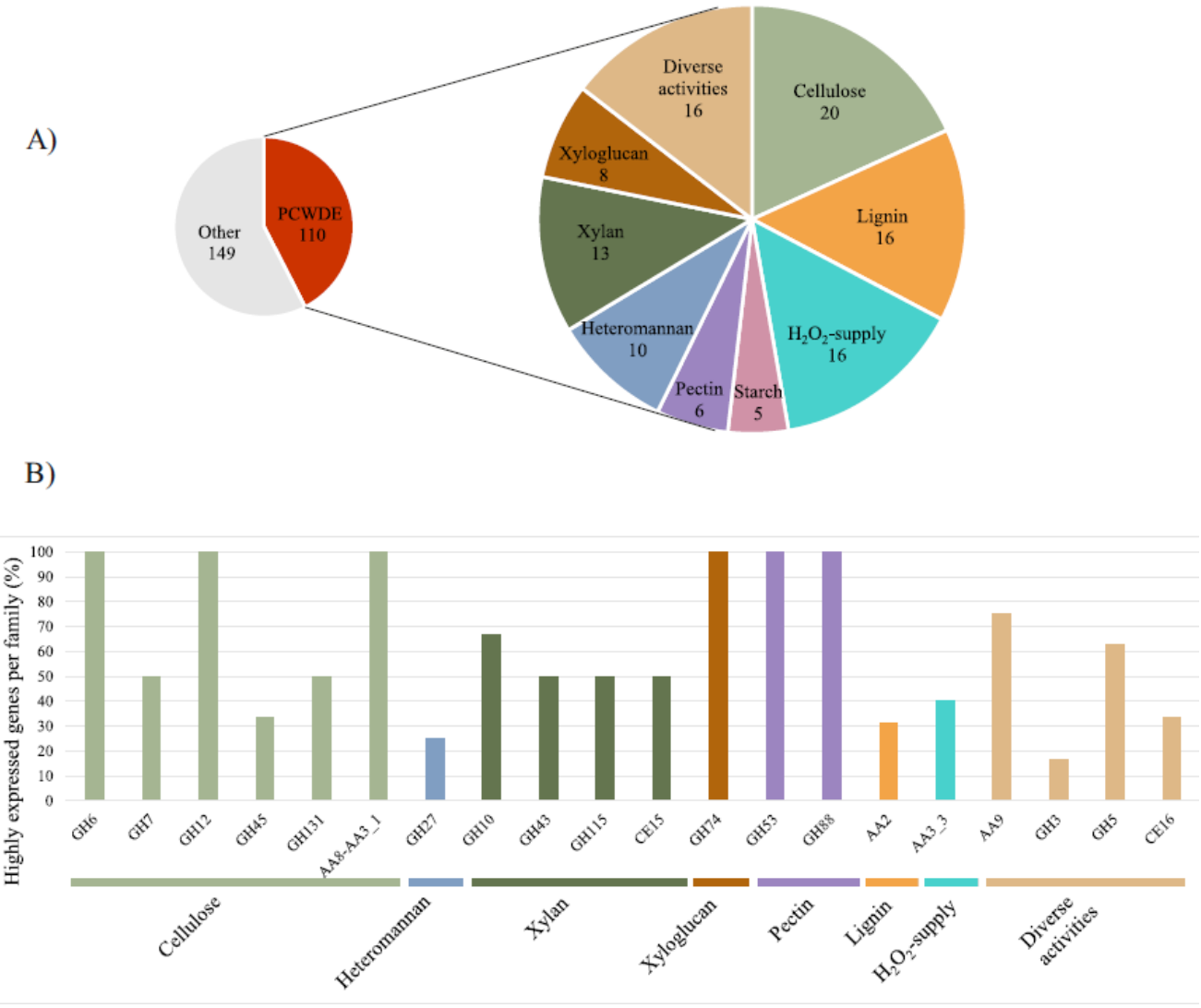

Figure 2. A) Functional distribution of detected putative CAZyme encoding genes identified in *O. rivulosa* spruce cultures. B) Highly expressed (>300 FKPM) putative CAZyme encoding genes per CAZy family as a percentage of total gene number per family. Substrates, the corresponding enzymes putatively act on, are indicated. PCWDE, plant cell wall degrading enzymes.

Figure 3. *O. rivulosa* monokaryon 3A-2 grown on solid spruce wood sticks for A) 2 weeks, B) 4 weeks and C) 8 weeks. D) Non-inoculated control cultivation.

Tables

Table 1. The highest expressed CAZyme encoding genes across 8-week cultivation of *O. rivulosa* on spruce. Only genes showing FPKM values higher than 1000 at any time point are presented.

			RNA level (FPKM)		
Protein ID	**CAZy family**	**Functional annotation**	**2 weeks**	**4 weeks**	**8 weeks**
806545	AA2	MnP	11194	21804	3071
835392	AA2	MnP	9970	19896	2638
641261	GH5_7	MAN	7664	257	116
838746	GH10	XLN	6589	176	28
821398	AA9	LPMO	4789	729	28
476379	CBM1-GH6	CBHII	4781	165	56
790443	AA3_3	AOX	4312	1889	551
731121	GH7-CBM1	CBHI	4121	287	50
727100	AA2	MnP	2938	803	85
833133	AA9-CBM1	LPMO	2878	439	70
788967	CBM1-GH5_5	EGL	2032	188	103
851185	GH10	XLN	1954	83	5
726082	GH12	EGL	1585	121	38
891614	AA2	MnP [*]	1565	174	2
749512	CE16	AE	1428	145	29
781628	AA9-CBM1	LPMO	1290	268	102
789780	CBM1-GH5_5	EGL	1268	152	73
812963	GH131	EGL	1211	79	24
719765	GH5_7	MAN	1201	43	29
724015	CE16	AE	1125	129	35

[*] (Hakala et al., 2006))

Supplementary files

Supplementary Figure 1. Principal component analysis (PCA) for *O. rivulosa* transcript counts. Two biological replicates used for the RNA-seq from 2-, 4-, and 8-week spruce wood cultivations are shown. O_2 and O_2.1, 2-week samples; O_4 and O_4.1, 4-week samples; O_8 and 5 O_8.1, 8-week samples.

Supplementary Figure 2. Sum of RNA levels (FPKM) detected in *O. rivulosa* spruce cultures during 8-week cultivation. Enzyme abbreviations are presented in Supplementary Table 2. Note that the y-scales of the graphs are not identical.

Supplementary Figure 3. Representation of sugar catabolic pathways, including expression profiles of the genes involved in the pathway. A) Glycolysis, mannose catabolism and TCA cycle. Enzymes in pale gray have no identified genes yet. B) Pentose catabolic- and pentose phosphate pathway. Enzymes in pale gray have no identified genes yet. C) L-rhamnose, D-galacturonic acid and Leloir D-galactose catabolic pathways. Enzymes in gray have no identified genes yet.

Supplementary Table 1. qRT-PCR primers used in this work.

Supplementary Table 2. Selected *O. rivulosa* CAZymes their substrates, abbreviations, EC numbers and the copy number of the corresponding genes.

Supplementary Table 3. Expressed genes encoding putative plant cell wall degrading CAZy, central carbon metabolism and fungal cell wall acting CAZy enzymes by *O. rivulosa* grown on solid spruce

633 wood during the time course of 8 weeks. A) Plant cell wall degrading CAZyme encoding genes. B)
634 Central carbon metabolism encoding genes involved in glycosis, mannose catabolism, TCA cycle, L-
635 rhamnose, D-galacturonic, Leloir, pentose catabolic and pentose phosphate pathways. C) Fungal cell
636 wall acting CAZyme encoding genes.

637 **Supplementary Table 1.** qRT-PCR primers used in this work.

Protein ID	Putative function	Enzyme abbreviation	Primer sequence (5' - 3')	Amplicon size (bp)	Primer efficiency E value (%)	Primer efficiency R^2 value
813284	β-1,4-Endoglucanase	EGL	F: GCGTATCTGGTGGAGAATGAG	108	99	0.999
			R: TGTACGCAGACGTAGTGAGG			
821398	Lytic polysaccharide monooxygenase	LPMO	F: TACCACCCTGGCTACTTCTC	267	97	0.998
			R: AGCCAATGTAGAACTGAGCAC			
806545	Manganese peroxidase	MnP	F: CGGTTACAAATTCACAAGTGTTGG	125	94	0.999
			R: AGGTTGTTCACACTGTCGTC			
727100	Manganese peroxidase	MnP	F: CGGTGAAGATACGCATGAGG	176	102	0.999
			R: GGAATCAAGTTGTTCACGGAG			
323916	Manganese peroxidase	MnP	F: TTTGACACGACTCCCTTCAC	247	101	0.999
			R: CTCTGTGCCATGAACTCCTG			
891614	Manganese peroxidase	MnP	F: TGAAGATGCACATGAAGCCA	172	96	0.998
			R: GTATCAGGTTGTTCACACTATCGT			
820050	Endopolygalacturonase	PGA	F: CCGTATCCAATGTGACCTATTCTG	130	98	0.994
			R: GAAGTTGATGTCCGAGACCT			
600970	Pectin methyl esterase	PME	F: CGTAACCTAGTACAAATCTGGGAC	161	104	0.993
			R: GGAATAGTTCGCAGCTAGATTCTC			
799009	β-1,4-Endoxylanase	XLN	F: CAGTCATCAATGCCTGTGTC	140	95	0.999
			R: GTTTCCTTACCAAGTTATCGTCC			
812492	Glyceraldehyde-3-phosphate dehydrogense	GAPDH	F: ACCCGTTCATCGACCTTGAG	230	99	0.999
			R: AATGAGCCTCAGCCTTCTCC			

638

639

640 **Supplementary Table 2.** Selected *O. rivulosa* CAZymes, their substrates, abbreviations, EC numbers

641 and the copy number of the corresponding genes.

CAZy family	Substrate	Abbreviation	Annotation	EC number	Copy no.
AA1_1	Lignin	LCC	Laccase	1.10.3.2	9
AA1_2	Lignin	FET	Ferroxidase	1.10.3.-	1
AA2	Lignin	MnP	Manganese peroxidase	1.11.1.13	11
AA2	Lignin	LiP	Lignin peroxidase	1.11.1.14	1
AA3_2	H_2O_2 supply	GOX	Glucose 1-oxidase	1.1.3.4	9

AA3_2	H_2O_2 supply	AAO	Aryl alcohol oxidase	1.1.3.7	6
AA3_3	H_2O_2 supply	AOX	Alcohol oxidase	1.1.3.13	5
AA5_1	H_2O_2 supply	GLX	Glyoxal oxidase	1.2.3.15	4
AA8-AA3_1	Cellulose	CDH	Cellobiose dehydrogenase	1.1.99.18	1
AA9	Cellulose	LPMO	Lytic polysaccharide monooxygenase	na	8
CE1	Hemicellulose (xylan)	AXE	Acetyl xylan esterase	3.1.1.72	2
CE8	Pectin	PME	Pectin methyl esterase	3.1.1.11	2
CE15	Hemicellulose (xylan)	GE	4-O-Methyl-glucuronyl methylesterase	3.1.1.-	2
CE16	Hemicellulose (xylan)	AE	Acetylesterase	3.1.1.6	9
GH1	Pectin (rhamnogalacturonan I)	LAC	β-1,4-Galactosidase	3.2.1.23	1
GH1	Cellulose	BGL	β-1,4-Glucosidase	3.2.1.21	2
GH2	Hemicellulose (heteromannan)	MND	β-1,4-Mannosidase	3.2.1.25	3
GH3	Cellulose	BGL	β-1,4-Glucosidase	3.2.1.21	5
GH3	Heteromannan	BXL	β-1,4-Xylosidase	3.2.1.37	1
GH5	Heteromannan	MAN	β-1,4-Endomannanase	3.2.1.78	1
GH5_5	Cellulose	EGL	β-1,4-Endoglucanase	3.2.1.4	2
GH5_7	Hemicellulose (heteromannan)	MAN	β-1,4-Endomannanase	3.2.1.78	2
GH5_22	Hemicellulose (heteromannan)	BXL	β-1,4-Xylosidase	3.2.1.37	2
GH5_31	Hemicellulose (heteromannan)	MAN	β-1,4-Endomannanase	3.2.1.78	1
GH6	Cellulose	CBHII	Cellobiohydrolase (non-reducing end)	3.2.1.91	1
GH7	Cellulose	CBHI	Cellobiohydrolase (reducing end)	3.2.1.176	2
GH10	Hemicellulose (xylan, xyloglucan)	XLN	β-1,4-Endoxylanase	3.2.1.8	6
GH12	Cellulose	EGL	β-1,4-Endoglucanase	3.2.1.4	2
GH13_1	Starch	AMY	α-Amylase	3.2.1.1	2
GH13_5	Starch	AMY	α-Amylase	3.2.1.1	1
GH15	Starch	GLA	Glucoamylase	3.2.1.3	3
GH27	Heteromannan	AGL	α-1,4-Galactosidase	3.2.1.22	4
GH28	Pectin	PGA	Endopolygalacturonase	3.2.1.15	1
GH28	Pectin	PGX	Exopolygalacturonase	3.2.1.67	1
GH28	Pectin	RGX	Exorhamnogalacturonase	3.2.1.-	2
GH31	Heteromannan	AGD	α-Glucosidase	3.2.1.22	5
GH31	Starch/Xyloglucan	AXL	α-Xylosidase	3.2.1.177	1
GH35	Pectin	LAC	β-1,4-Galactosidase	3.2.1.23	1
GH43	Pectin	ABN	Endoarabinanase	3.2.1.99	2
GH45	Cellulose	EGL	β-1,4-Endoglucanase	3.2.1.4	3
GH51	Pectin	ABF	α-Arabinofuranosidase	3.2.1.55	2
GH53	Pectin	GAL	β-1,4-Endogalactanase	3.2.1.89	1
GH74	Xylan/ Xyloglucan	XG-EG	Xyloglucanase	3.2.1.151	1
GH78	Pectin	RHA	α-Rhamnosidase	3.2.1.40	1
GH88	Pectin	UGH	Unsaturated glucuronyl hydrolase	3.2.1.-	1
GH95	Xylan/ Xyloglucan	AFC	α-L-Fucosidase	3.2.1.51	1

GH115	Xylan/ Xyloglucan	AGU	α-Glucuronidase	3.2.1.139	2
GH127	Pectin	ABF	α-Arabinofuranosidase	3.2.1.55	1
GH131	Cellulose/ β-1,3/ β-1,6 glucans	EGL	β-1,4-Endoglucanase	3.2.1.4	2

642

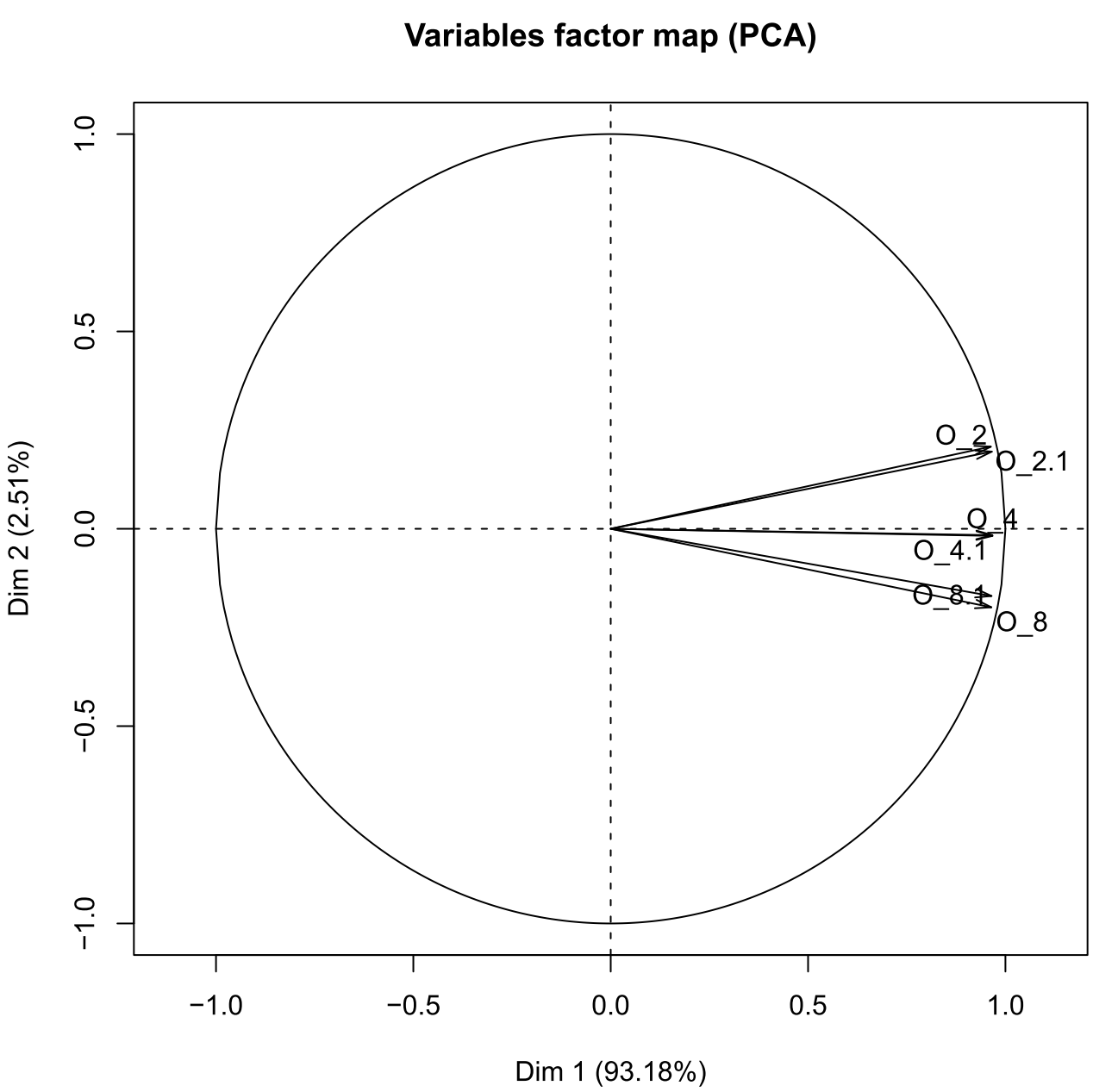

Supplementary Figure 1. Principal component analysis (PCA) for *O. rivulosa* transcript counts. Two biological replicates used for the RNA-seq from 2-, 4-, and 8-week spruce wood cultivations are shown. Principal component 1 (Dim 1) and principle component 2 (Dim 2) explain 93.18% and 2.51% of variance, respectively. O_2 and O_2.1, 2-week samples; O_4 and O_4.1, 4-week samples; O_8 and O_8.1, 8-week samples.

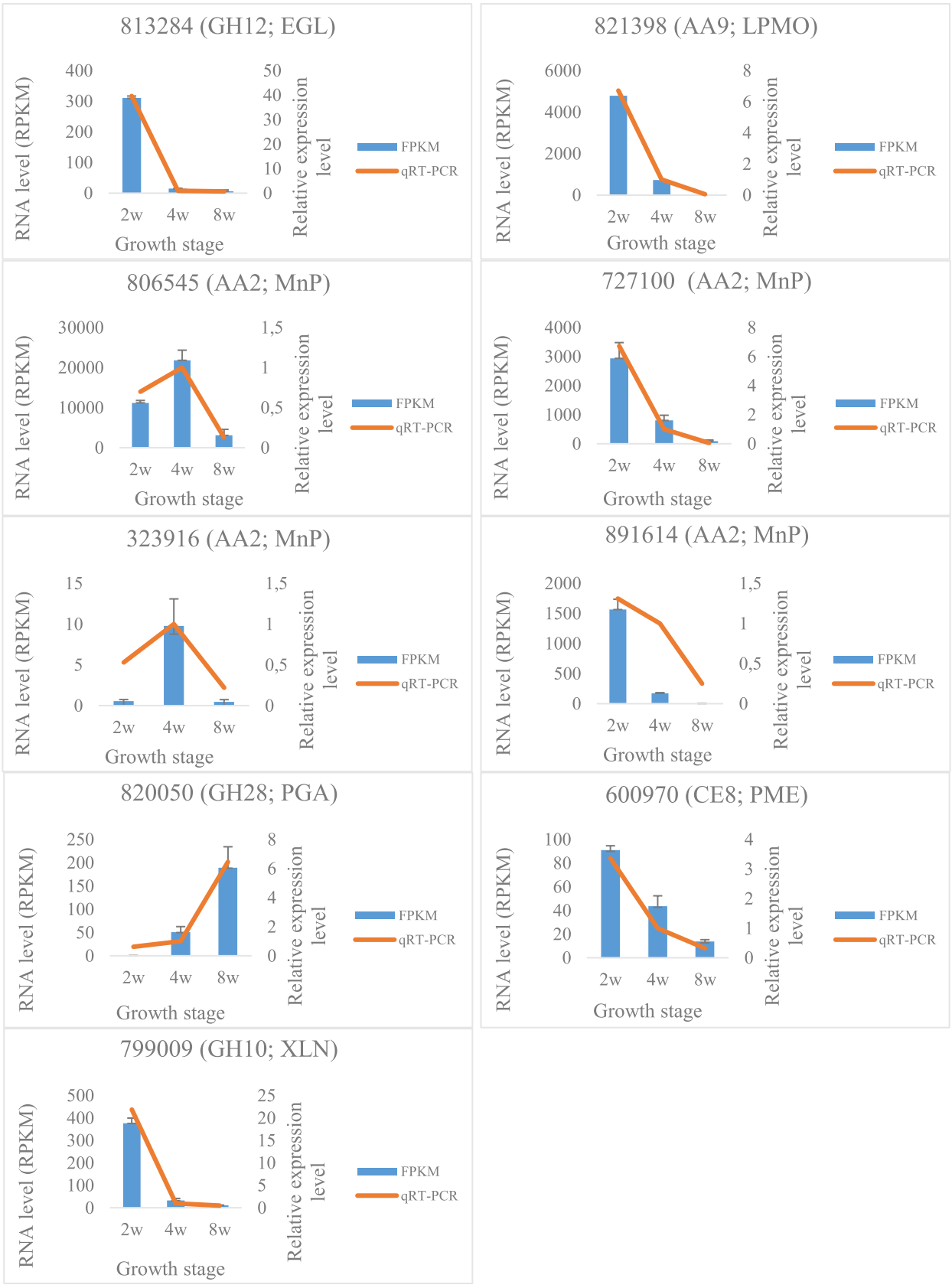

Supplementary Figure 2. Validation of RNA-seq analysis by qRT-PCR of nine selected genes involved in plant cell wall degradation in *O. rivulosa*. Columns represent RNA level (FPKM), lines represent qRT-PCR values (relative unit). Error bars represent standard deviation of two biological replicates and three replicate qRT-PCR reactions. Enzyme abbreviations are presented in Supplementary Table 2.

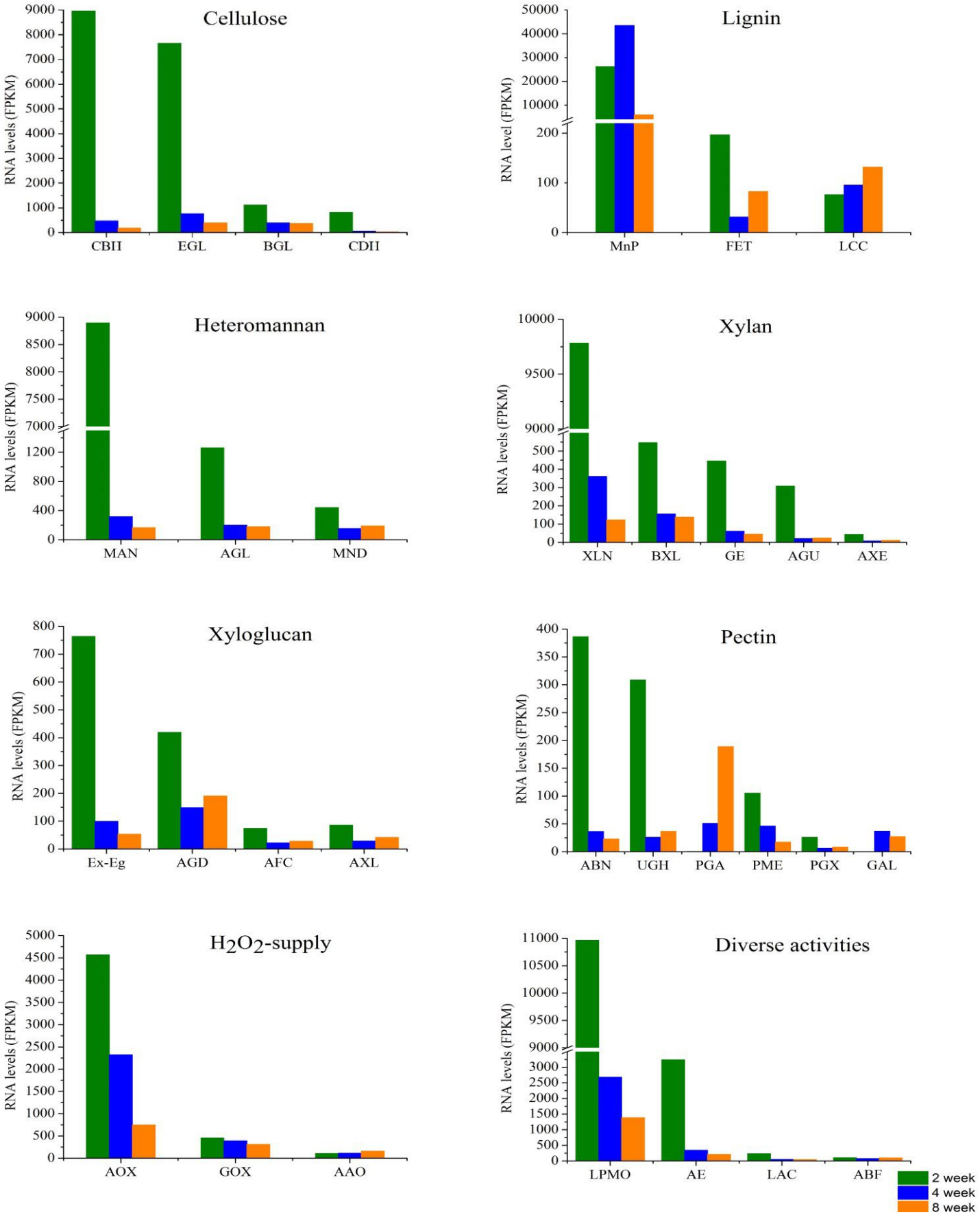

Supplementary Figure 3. Sum of RNA levels (FPKM) detected in *O. rivulosa* spruce cultures during 8-week cultivation. Enzyme abbreviations are presented in Supplementary Table 2. Note that the y-scales of the graphs are not identical.

Supplementary Figure 4. Representation of sugar catabolic pathways, including expression profiles of the genes involved in the pathways. A) Glycolysis, mannose catabolism and TCA cycle. Enzymes in pale grey have no identified genes yet.

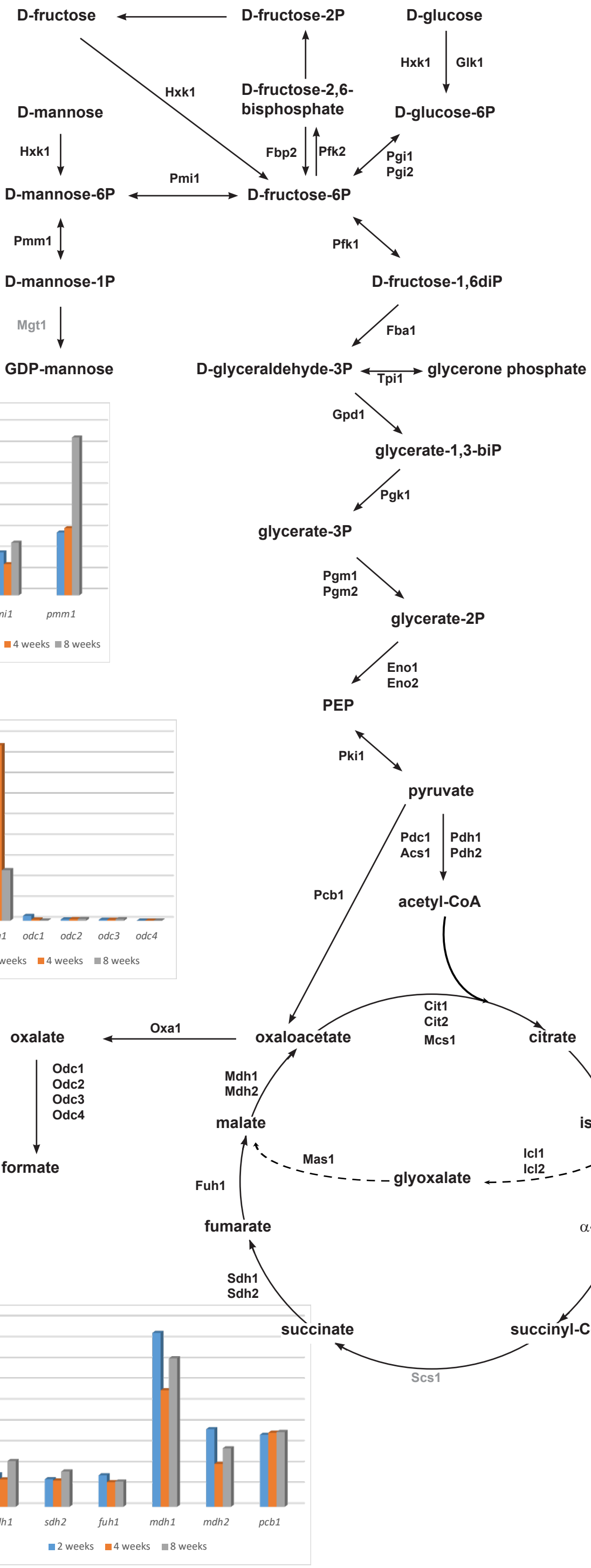

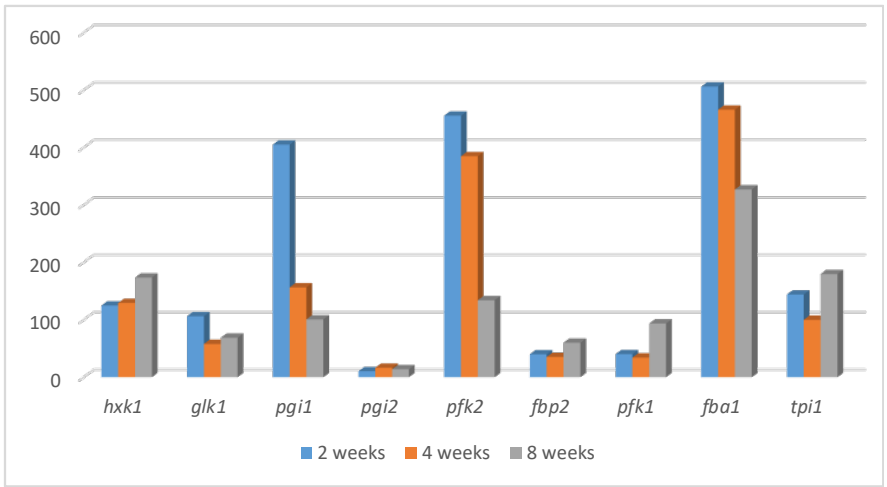

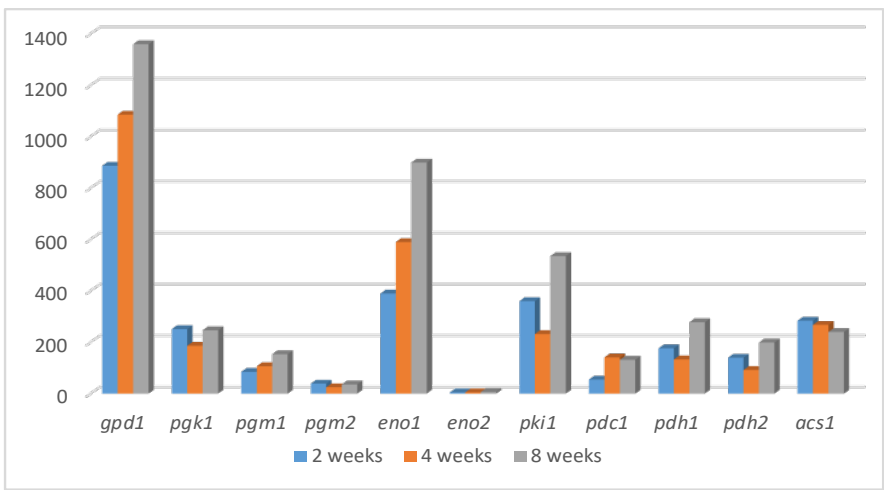

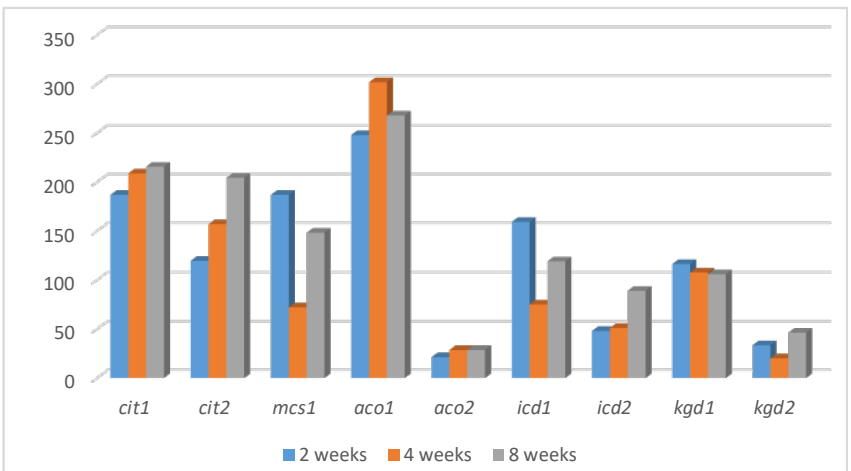

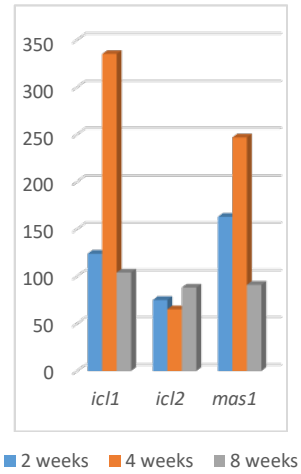

Supplementary Figure 4. B) Pentose catabolic and pentose phosphate pathway. Enzymes in pale grey have no identified genes yet.

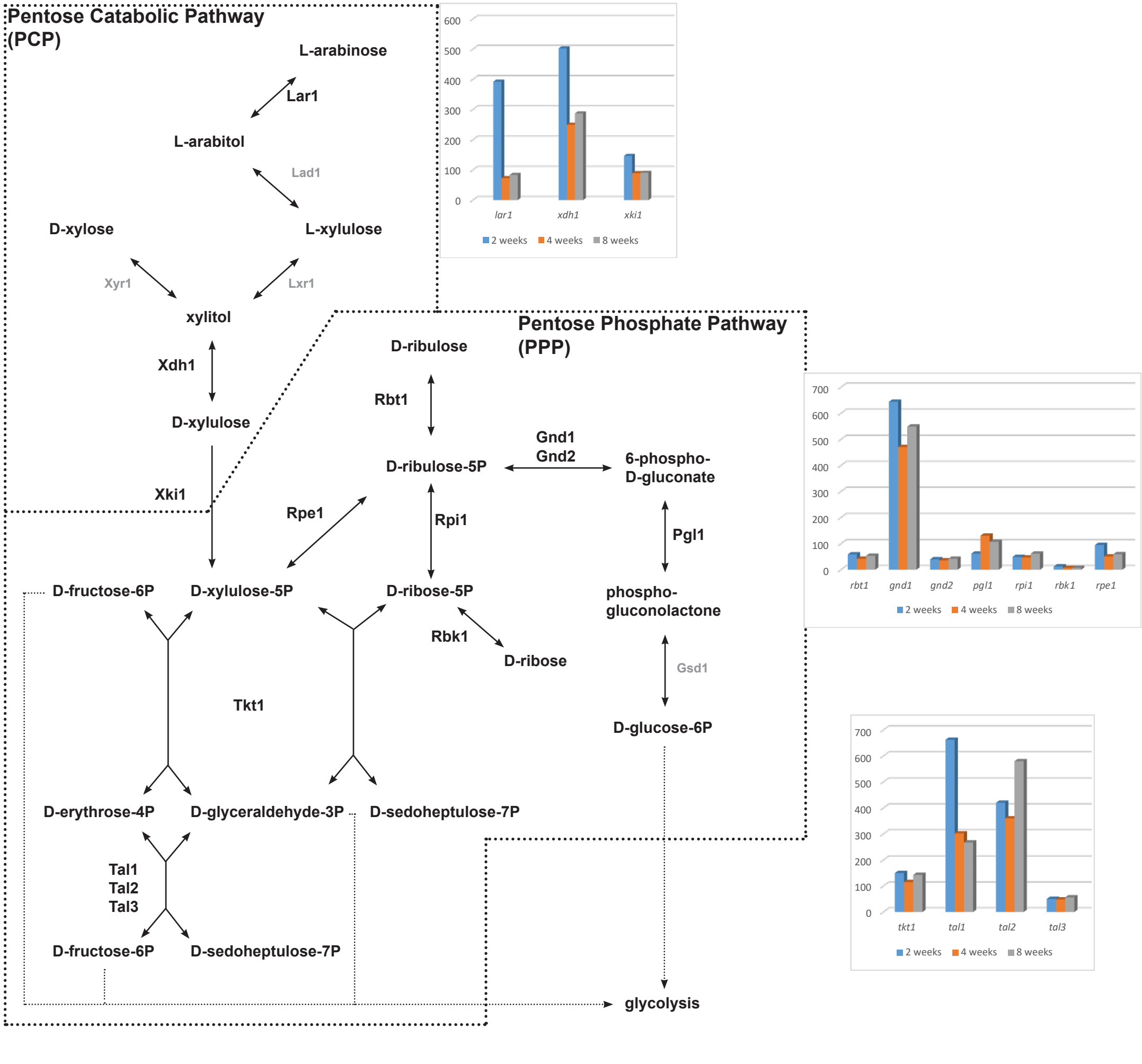

Supplementary Figure 4. C) L-rhamnose, D-galacturonic acid and Leloir D-galactose catabolic pathways. Enzymes in pale grey have no identified genes yet.

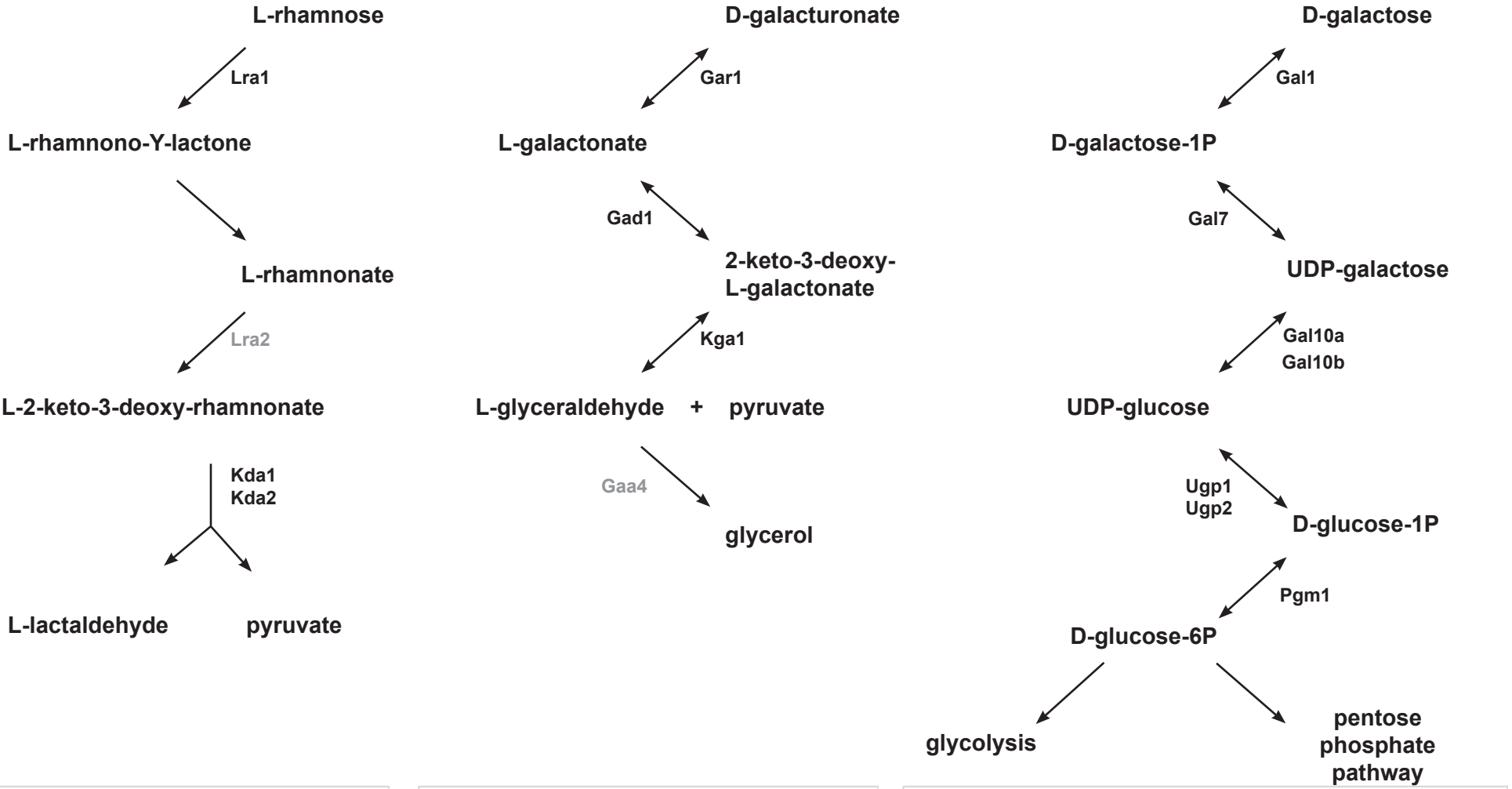

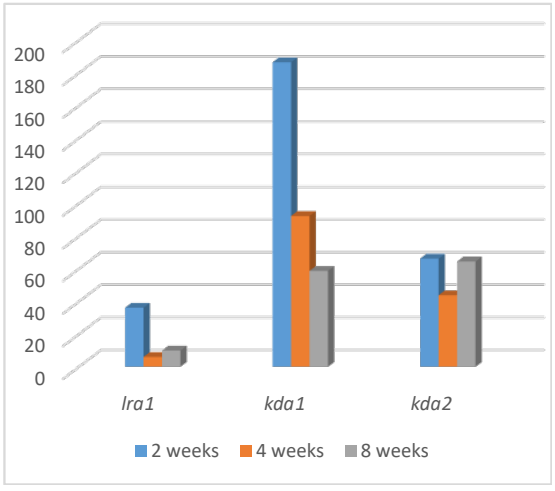

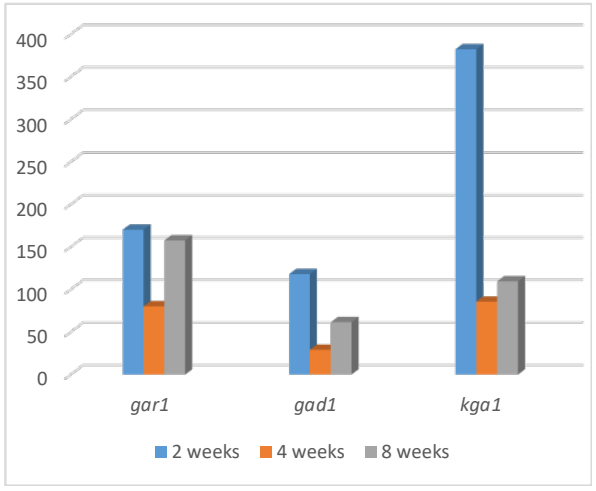

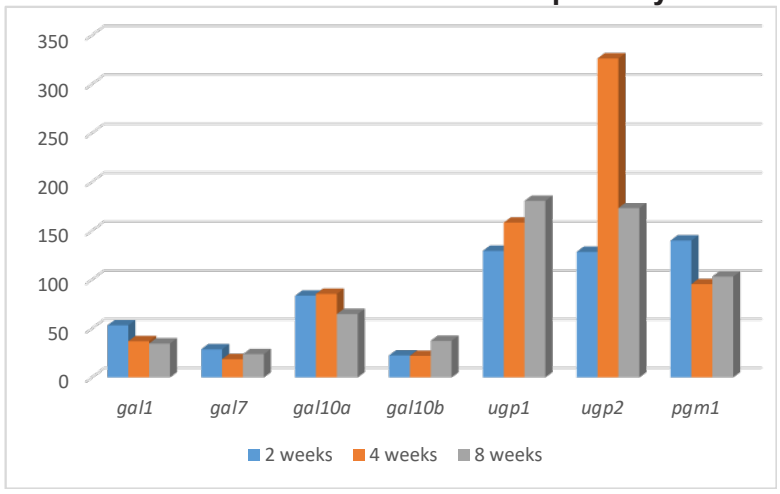

Supplementary Table 3. Expressed genes encoding putative plant cell wall degrading CAZy, central carbo
A) Plant cell wall degrading CAZyme encoding genes.
Enzyme abbreviations: AAO = aryl alcohol oxidase, ABF = α-arabinofuranosidase, ABN = endoarabinanas
AXL = α-xylosidase, BGL = β-1,4-glucosidase, BQR = benzoquinone reductase, BXL = β-1,4-xylosidase,
GAL = β-1,4-endogalactanase, GE = 4-O-methyl-glucuronyl methylesterase, GLA = glucoamylase, GLX =
LCC = laccase, LiP = lignin peroxidase, PGA = endopolygalacturonase, PGX = exopolygalacturonase, PM
XLN = β-1,4-endoxylanase

Protein ID	CAZy family	Enzyme abbreviation	Substrate	Functional annotation
596333	AA1	LCC	lignin	Multicopper oxidase
726849	AA1_1	LCC	lignin	Multicopper oxidase
814238	AA1_1	LCC	lignin	Multicopper oxidase
875588	AA1_1	LCC	lignin	Multicopper oxidase
890919	AA1_1	LCC	lignin	Multicopper oxidase
736636	AA1_1	LCC	lignin	Multicopper oxidase
452017	AA1_1	LCC	lignin	Multicopper oxidase
741387	AA1_1	LCC	lignin	Multicopper oxidase
867863	AA1_1	LCC	lignin	Multicopper oxidase
796512	AA1_2	FET	lignin	Multicopper oxidase
806545	AA2_frag	MnP	lignin	Class II peroxidase
835392	AA2_frag	MnP	lignin	Class II peroxidase
727100	AA2	MnP	lignin	Class II peroxidase
891614	AA2	MnP	lignin	Class II peroxidase
438941	AA2	MnP	lignin	Class II peroxidase
729972	AA2	MnP	lignin	Class II peroxidase
60162	AA2	MnP	lignin	Class II peroxidase
323916	AA2	MnP	lignin	Class II peroxidase
511960	AA2	MnP	lignin	Class II peroxidase
412406	AA2	MnP	lignin	Class II peroxidase
825700	AA2	MnP	lignin	Class II peroxidase
803460	AA2	LiP	lignin	Class II peroxidase
835715	AA2_frag		lignin	Class II peroxidase
835716	AA2		lignin	Class II peroxidase
813497	AA2_frag		lignin	Class II peroxidase
770945	AA2_cyt	CPO	lignin	Class II peroxidase
725321	AA3_2	AAO	H_2O_2-supply	GMC oxidoreductase
773345	AA3_2	AAO	H_2O_2-supply	GMC oxidoreductase
795098	AA3_2	AAO	H_2O_2-supply	GMC oxidoreductase
735182	AA3_2	AAO	H_2O_2-supply	GMC oxidoreductase
837570	AA3_2	AAO	H_2O_2-supply	GMC oxidoreductase
885712	AA3_2	GOX	H_2O_2-supply	GMC oxidoreductase
769671	AA3_2	GOX	H_2O_2-supply	GMC oxidoreductase
789242	AA3_2	GOX	H_2O_2-supply	GMC oxidoreductase
804770	AA3_2	GOX	H_2O_2-supply	GMC oxidoreductase
815690	AA3_2	GOX	H_2O_2-supply	GMC oxidoreductase
829135	AA3_2	GOX	H_2O_2-supply	GMC oxidoreductase
731504	AA3_2	GOX	H_2O_2-supply	GMC oxidoreductase
732948	AA3_2	GOX	H_2O_2-supply	GMC oxidoreductase

830066	AA3_2_frag	GOX	H_2O_2-supply	GMC oxidoreductase
790443	AA3_3	AOX	H_2O_2-supply	GMC oxidoreductase
814600	AA3_3	AOX	H_2O_2-supply	GMC oxidoreductase
564635	AA3_3	AOX	H_2O_2-supply	GMC oxidoreductase
875460	AA3_3	AOX	H_2O_2-supply	GMC oxidoreductase
792863	AA3_3	AOX	H_2O_2-supply	GMC oxidoreductase
35182	AA5_1	GLX	H_2O_2-supply	Copper radical oxidase
826706	AA5_1	GLX	H_2O_2-supply	Copper radical oxidase
759764	AA5_1	GLX	H_2O_2-supply	Copper radical oxidase
661935	AA5_1	GLX	H_2O_2-supply	Copper radical oxidase
795134	AA6	BQR	lignin	Benzoquinone reductase
664751	AA8-AA3_1	CDH	cellulose	Iron reductase domain / GMC
821398	AA9	LPMO	diverse	Lytic polysaccharide monooxy
799019	AA9	LPMO	diverse	Lytic polysaccharide monooxy
796835	AA9	LPMO	diverse	Lytic polysaccharide monooxy
519691	AA9	LPMO	diverse	Lytic polysaccharide monooxy
794851	AA9	LPMO	diverse	Lytic polysaccharide monooxy
739314	AA9	LPMO	diverse	Lytic polysaccharide monooxy
833133	AA9-CBM1	LPMO	diverse	Lytic polysaccharide monooxy
781628	AA9-CBM1	LPMO	diverse	Lytic polysaccharide monooxy
792896	CBM1-CE1	AXE	xylan	Carbohydrate-Binding Module
260257	CBM1-CE1	AXE	xylan	Carbohydrate-Binding Module
600970	CE8	PME	pectin	Carbohydrate Esterase Family
793338	CE8	PME	pectin	Carbohydrate Esterase Family
762191	CE15	GE	xylan	Carbohydrate Esterase Family
721831	CE15	GE	xylan	Carbohydrate Esterase Family
816606	CE16	AE	diverse	Carbohydrate Esterase Family
724015	CE16	AE	diverse	Carbohydrate Esterase Family
861019	CE16	AE	diverse	Carbohydrate Esterase Family
864632	CE16	AE	diverse	Carbohydrate Esterase Family
815252	CE16	AE	diverse	Carbohydrate Esterase Family
797374	CE16	AE	diverse	Carbohydrate Esterase Family
797388	CE16	AE	diverse	Carbohydrate Esterase Family
890618	CE16	AE	diverse	Carbohydrate Esterase Family
749512	CBM1-CE16	AE	diverse	Carbohydrate-Binding Module
889978	GH1	LAC	diverse	Glycoside Hydrolase Family 1
731281	GH1	BGL	cellulose	Glycoside Hydrolase Family 1
770661	GH1	BGL	cellulose	Glycoside Hydrolase Family 1
813927	GH2	MND	heteromannan	Glycoside Hydrolase Family 2
753990	GH2	MND	heteromannan	Glycoside Hydrolase Family 2
815162	GH2	MND	heteromannan	Glycoside Hydrolase Family 2
14692	GH3	BGL	cellulose	Glycoside Hydrolase Family 3
784936	GH3	BGL	cellulose	Glycoside Hydrolase Family 3
627233	GH3	BGL	cellulose	Glycoside Hydrolase Family 3
627302	GH3	BGL	cellulose	Glycoside Hydrolase Family 3
788396	GH3	BGL	cellulose	Glycoside Hydrolase Family 3
337845	GH3	BXL	xylan	Glycoside Hydrolase Family 3
273202	GH5	MAN	heteromannan	Glycoside Hydrolase Family 5
789780	CBM1-GH5_5	EGL	cellulose	Carbohydrate-Binding Module

788967	CBM1-GH5_5	EGL	cellulose	Carbohydrate-Binding Module
641261	CBM1-GH5_7	MAN	heteromannan	Carbohydrate-Binding Module
719765	GH5_7	MAN	heteromannan	Glycoside Hydrolase Family 5
819531	GH5_22	BXL	xylan	Glycoside Hydrolase Family 5
826236	GH5_22	BXL	xylan	Glycoside Hydrolase Family 5
814478	GH5_31	MAN	heteromannan	Glycoside Hydrolase Family 5
476379	CBM1-GH6	CBHII	cellulose	Carbohydrate-Binding Module
731121	GH7-CBM1	CBHI	cellulose	Glycoside Hydrolase Family 7
91658	GH7-CBM1	CBHI	cellulose	Glycoside Hydrolase Family 7
799009	GH10	XLN	xylan	Glycoside Hydrolase Family 10
782683	GH10	XLN	xylan	Glycoside Hydrolase Family 10
786094	GH10	XLN	xylan	Glycoside Hydrolase Family 10
851185	CBM1-GH10	XLN	xylan	Carbohydrate-Binding Module
838746	CBM1-GH10	XLN	xylan	Carbohydrate-Binding Module
762583	CBM1-GH10	XLN	xylan	Carbohydrate-Binding Module
813284	GH12	EGL	cellulose	Glycoside Hydrolase Family 12
726082	GH12	EGL	cellulose	Glycoside Hydrolase Family 12
616587	GH13_1	AMY	starch	Glycoside Hydrolase Family 13
735014	GH13_1	AMY	starch	Glycoside Hydrolase Family 13
789297	GH13_5	AMY	starch	Glycoside Hydrolase Family 13
833127	GH15	GLA	starch	Glycoside Hydrolase Family 15
812469	GH15-CBM20	GLA	starch	Glycoside Hydrolase Family 15
791064	GH15-CBM20	GLA	starch	Glycoside Hydrolase Family 15
849432	GH27	AGL	heteromannan	Glycoside Hydrolase Family 27
810034	GH27	AGL	heteromannan	Glycoside Hydrolase Family 27
13793	GH27	AGL	heteromannan	Glycoside Hydrolase Family 27
849398	GH27	AGL	heteromannan	Glycoside Hydrolase Family 27
820050	GH28	PGA	pectin	Glycoside Hydrolase Family 28
206352	GH28	PGX	pectin	Glycoside Hydrolase Family 28
875830	GH28	RGX	pectin	Glycoside Hydrolase Family 28
793237	GH28	RGX	pectin	Glycoside Hydrolase Family 28
169586	GH31	AGD	xyloglucan	Glycoside Hydrolase Family 31
891711	GH31	AGD	xyloglucan	Glycoside Hydrolase Family 31
736445	GH31	AGD	xyloglucan	Glycoside Hydrolase Family 31
837500	GH31	AGD	xyloglucan	Glycoside Hydrolase Family 31
793998	GH31	AGD	xyloglucan	Glycoside Hydrolase Family 31
788201	GH31	AXL	xyloglucan	Glycoside Hydrolase Family 31
789567	GH35	LAC	diverse	Glycoside Hydrolase Family 35
729166	GH43	ABN	pectin	Glycoside Hydrolase Family 43
548101	GH43	ABN	pectin	Glycoside Hydrolase Family 43
834143	GH45	EGL	cellulose	Glycoside Hydrolase Family 45
753033	GH45	EGL	cellulose	Glycoside Hydrolase Family 45
773627	GH45	EGL	cellulose	Glycoside Hydrolase Family 45
790347	GH51	ABF	diverse	Glycoside Hydrolase Family 51
760626	GH51	ABF	diverse	Glycoside Hydrolase Family 51
723211	GH53	GAL	pectin	Glycoside Hydrolase Family 53
808997	GH74	XG-EG	xyloglucan	Glycoside Hydrolase Family 74
735541	GH78	RHA	pectin	Glycoside Hydrolase Family 78
815167	GH88	UGH	pectin	Glycoside Hydrolase Family 88
738866	GH95	AFC	xyloglucan	Glycoside Hydrolase Family 95

726547	GH115	AGU	xylan	Glycoside Hydrolase Family 11
742368	GH115	AGU	xylan	Glycoside Hydrolase Family 11
832165	GH127	ABF	diverse	Glycoside Hydrolase Family 12
812963	GH131	EGL	cellulose	Glycoside Hydrolase Family 13
812977	GH131	EGL	cellulose	Glycoside Hydrolase Family 13

n metabolism and fungal cell wall acting CAZy enzymes by *O. rivulosa* grown on solid spruce wood during

e, AE = acetylesterase, AFC = α-L-fucosidase, AGD = α-glucosidase, AGL = α-1,4-galactosidase, AGU =
CBHI = cellobiohydrolase (reducing end), CBHII = cellobiohydrolase (non-reducing end), CPO = chloroper
glyoxal oxidase, GOX = glucose oxidase, LAC = β-1,4-galactosidase, LPMO = lytic polysaccharide mono
E = pectin methyl esterase, RGX = exorhamnogalacturonase, RHA = α-rhamnosidase, UGH = unsaturated

Time point (FPKM)			Comparison			
2 weeks	**4 weeks**	**8 weeks**	**4 weeks_over 2 weeks**	**p-value**	**4 weeks_over 8 weeks**	**p-value**
20,6	11,8	15,9	0,6	0,1	0,7	0,2
12,2	2,8	2,8	0,2	0,1	1,0	1,0
1,0	1,9	1,2	1,9	0,2	1,6	0,3
11,8	44,1	13,9	3,8	0,0	3,2	0,0
2,2	1,3	2,7	0,6	0,4	0,5	0,2
12,4	17,3	16,9	1,4	0,0	1,0	0,7
6,1	7,4	10,0	1,2	0,3	0,7	0,1
1,3	1,6	2,6	1,2	0,6	0,6	0,2
9,0	7,4	65,9	0,8	0,3	0,1	0,0
196,5	31,5	82,8	0,2	0,0	0,4	0,0
11193,5	21803,9	3070,7	1,9	0,0	7,1	0,0
9970,3	19896,3	2637,6	2,0	0,0	7,5	0,0
2937,9	802,6	85,2	0,3	0,0	9,4	0,0
1564,9	174,4	1,8	0,1	0,0	98,3	0,0
311,3	321,8	28,0	1,0	0,9	11,5	0,2
139,4	294,4	45,7	2,1	0,0	6,4	0,0
85,7	153,9	25,9	1,8	0,0	5,9	0,0
0,5	9,8	0,5	17,9	0,1	21,0	0,1
21,7	21,1	22,0	1,0	0,8	1,0	0,8
1,4	9,5	2,6	7,0	0,0	3,6	0,0
0,9	4,1	1,3	4,6	0,1	3,1	0,1
3,8	4,0	4,0	1,0	0,9	1,0	1,0
7,2	5,3	7,0	0,7	0,4	0,8	0,1
8,5	12,9	48,6	1,5	0,1	0,3	0,0
3,1	2,2	5,1	0,7	0,4	0,4	0,1
20,0	22,5	106,8	1,1	0,2	0,2	0,0
15,9	10,5	11,7	0,7	0,1	0,9	0,4
22,0	18,6	16,3	0,8	0,0	1,1	0,1
12,3	22,3	15,7	1,8	0,0	1,4	0,1
31,7	32,4	51,4	1,0	0,7	0,6	0,0
24,5	28,7	63,9	1,2	0,1	0,4	0,0
229,3	85,5	68,6	0,4	0,0	1,2	0,4
35,3	40,7	20,1	1,2	0,2	2,0	0,0
71,2	50,3	48,9	0,7	0,2	1,0	0,9
72,6	96,7	69,1	1,3	0,4	1,4	0,4
15,7	30,8	30,2	2,0	0,0	1,0	0,9
4,2	6,4	8,2	1,5	0,4	0,8	0,6
1,9	3,3	4,6	1,7	0,2	0,7	0,3
15,2	67,4	51,8	4,4	0,0	1,3	0,2

10,6	9,9	9,6	0,9	0,5	1,0	0,9
4312,1	1888,8	551,3	0,4	0,0	3,4	0,1
168,6	382,7	142,0	2,3	0,4	2,7	0,4
65,4	49,3	36,4	0,8	0,1	1,4	0,0
1,6	2,5	2,7	1,6	0,1	0,9	0,7
19,4	10,8	13,1	0,6	0,0	0,8	0,3
180,5	144,0	136,0	0,8	0,0	1,1	0,5
72,2	69,9	71,2	1,0	0,8	1,0	0,9
1,7	1,1	1,8	0,7	0,3	0,6	0,3
20,3	46,0	118,1	2,3	0,0	0,4	0,0
610,1	828,5	447,7	1,4	0,1	1,9	0,0
816,0	59,9	25,5	0,1	0,0	2,3	0,0
4788,7	729,3	28,4	0,2	0,1	25,7	0,0
450,7	60,5	13,3	0,1	0,0	4,5	0,0
665,1	283,2	146,7	0,4	0,2	1,9	0,1
18,4	20,1	19,4	1,1	0,4	1,0	0,8
870,9	864,0	986,4	1,0	0,9	0,9	0,3
3,6	15,7	18,1	4,4	0,1	0,9	0,6
2877,9	439,4	69,6	0,2	0,0	6,3	0,0
1290,2	268,4	102,5	0,2	0,0	2,6	0,0
26,1	4,8	8,8	0,2	0,0	0,5	0,3
17,2	3,2	2,0	0,2	0,1	1,6	0,0
90,9	43,5	13,7	0,5	0,0	3,2	0,0
14,3	2,6	3,5	0,2	0,0	0,7	0,2
408,3	47,3	29,1	0,1	0,0	1,6	0,1
37,7	13,8	15,5	0,4	0,1	0,9	0,6
504,4	4,0	10,0	0,0	0,0	0,4	0,2
1125,4	129,0	35,3	0,1	0,0	3,6	0,0
2,4	1,3	1,4	0,5	0,1	1,0	0,9
132,3	28,4	78,5	0,2	0,0	0,4	0,2
11,5	8,9	9,1	0,8	0,3	1,0	0,9
2,8	3,4	3,5	1,2	0,6	1,0	0,9
20,8	14,8	28,8	0,7	0,1	0,5	0,0
11,8	10,1	16,5	0,9	0,6	0,6	0,1
1428,0	145,3	29,1	0,1	0,0	5,0	0,0
79,5	21,7	21,8	0,3	0,0	1,0	0,9
255,2	105,8	102,0	0,4	0,0	1,0	0,9
124,3	86,7	86,5	0,7	0,1	1,0	1,0
158,7	12,4	30,3	0,1	0,0	0,4	0,1
283,3	112,9	129,8	0,4	0,0	0,9	0,5
0,0	29,1	30,0	0,6	0,1	1,0	0,9
324,7	62,1	15,7	0,2	0,1	3,9	0,0
137,9	26,3	20,7	0,2	0,0	1,3	0,4
165,4	23,2	53,5	0,1	0,0	0,4	0,0
24,7	9,3	18,4	0,4	0,1	0,5	0,0
84,8	74,3	77,1	0,9	0,5	1,0	0,9
175,3	31,9	31,7	0,2	0,0	1,0	1,0
22,8	9,0	7,6	0,4	0,1	1,2	0,6
1268,0	151,7	73,5	0,1	0,0	2,1	0,1

2031,6	187,7	103,4	0,1	0,0	1,8	0,2
7663,8	257,4	115,6	0,0	0,0	2,2	0,1
1201,0	43,3	29,0	0,0	0,0	1,5	0,1
185,6	62,0	53,3	0,3	0,0	1,2	0,6
50,2	19,8	23,9	0,4	0,0	0,8	0,4
7,1	8,2	14,3	1,2	0,4	0,6	0,0
4780,7	165,0	56,0	0,0	0,0	2,9	0,1
4121,5	287,4	50,3	0,1	0,0	5,7	0,0
50,4	19,7	75,4	0,4	0,1	0,3	0,1
376,4	32,8	11,2	0,1	0,0	2,9	0,1
57,0	5,1	5,2	0,1	0,0	1,0	1,0
105,0	17,1	17,4	0,2	0,0	1,0	0,9
1954,5	82,5	4,9	0,0	0,0	17,0	0,0
6588,6	176,3	28,0	0,0	0,0	6,3	0,0
702,0	47,5	56,7	0,1	0,0	0,8	0,8
310,7	14,7	6,1	0,0	0,0	2,4	0,1
1584,7	121,2	37,7	0,1	0,1	3,2	0,1
33,1	50,5	97,8	1,5	0,1	0,5	0,0
65,9	65,2	278,6	1,0	0,9	0,2	0,0
14,3	6,5	18,0	0,5	0,0	0,4	0,0
42,0	24,4	45,1	0,6	0,1	0,5	0,1
186,9	22,6	51,6	0,1	0,0	0,4	0,1
66,0	21,7	162,5	0,3	0,0	0,1	0,1
905,7	52,7	56,0	0,1	0,0	0,9	0,8
149,5	24,1	13,2	0,2	0,0	1,8	0,0
121,3	12,7	29,7	0,1	0,0	0,4	0,2
84,9	109,8	80,8	1,3	0,4	1,4	0,4
0,5	50,9	189,1	93,4	0,0	0,3	0,1
25,9	6,1	8,5	0,2	0,0	0,7	0,0
18,7	10,3	9,7	0,6	0,1	1,1	0,5
9,1	2,7	5195,0	0,3	0,0	0,5	0,2
121,8	6,2	14,4	0,1	0,0	0,4	0,1
59,7	8,1	11,7	0,1	0,0	0,7	0,4
161,6	42,8	71,6	0,3	0,0	0,6	0,2
17,1	31,5	18,8	1,8	0,0	1,7	0,0
59,0	59,9	74,3	1,0	0,3	0,8	0,0
85,7	29,0	41,8	0,3	0,0	0,7	0,3
154,0	30,1	19,2	0,2	0,0	1,6	0,1
375,4	16,7	11,6	0,0	0,0	1,4	0,1
11,1	19,8	11,4	1,8	0,0	1,7	0,1
123,6	11,8	1,0	0,1	0,0	11,8	0,1
846,7	25,3	8,6	0,0	0,0	2,9	0,0
126,1	131,2	106,7	1,0	0,5	1,2	0,1
0,0	14,9	13,7	0,1	0,0	1,1	0,3
85,9	33,4	38,5	0,4	0,0	0,9	0,4
0,0	36,9	27,1	0,0	0,0	1,4	0,1
763,9	99,6	53,2	0,1	0,0	1,9	0,1
14,0	7,7	8,6	0,6	0,0	0,9	0,3
308,6	26,0	36,7	0,1	0,0	0,7	0,1
73,7	22,1	28,0	0,3	0,0	0,8	0,2

300,3	17,5	15,6	0,1	0,0	1,1	0,5
7,7	3,5	8,7	0,4	0,1	0,4	0,1
14,7	29,2	43,4	2,0	0,2	0,7	0,2
1211,2	78,8	23,8	0,1	0,0	3,3	0,0
144,5	45,2	33,9	0,3	0,0	1,3	0,3

g the time course of 8 weeks.

α-glucuronidase, AMY = α-amylase, AOX = alcohol oxidase, AXE = acetyl xylan esterase,
roxidase, CDH = cellobiose dehydrogenase, EGL = β-1,4-edoglucanase, FET = ferroxidase
oxygenase, MAN = β-1,4-endomannanase, MND = β-1,4-mannosidase, MnP = manganese peroxidase,
glucuronyl hydrolase, XG-EG = xyloglucanase

2 weeks_over 8 weeks	p-value
1,3	0,3
4,3	0,1
0,9	0,7
0,8	0,5
0,8	0,5
0,7	0,1
0,6	0,0
0,5	0,2
0,1	0,0
2,4	0,0
3,6	0,0
3,8	0,0
34,5	0,0
881,6	0,0
11,1	0,0
3,0	0,0
3,3	0,0
1,2	0,8
1,0	1,0
0,5	0,0
0,7	0,4
0,9	0,9
1,0	0,9
0,2	0,0
0,6	0,2
0,2	0,0
1,4	0,1
1,3	0,0
0,8	0,3
0,6	0,0
0,4	0,0
3,3	0,0
1,8	0,0
1,5	0,0
1,1	0,7
0,5	0,0
0,5	0,1
0,4	0,0
0,3	0,0

1,1	0,7
7,8	0,0
1,2	0,5
1,8	0,0
0,6	0,1
1,5	0,1
1,3	0,0
1,0	0,8
1,0	1,0
0,2	0,0
1,4	0,1
32,0	0,0
168,4	0,1
33,8	0,0
4,5	0,1
0,9	0,8
0,9	0,1
0,2	0,0
41,3	0,0
12,6	0,0
3,0	0,0
8,6	0,0
6,6	0,0
4,1	0,0
14,0	0,0
2,4	0,1
50,6	0,0
31,8	0,0
1,8	0,2
1,7	0,2
1,3	0,1
0,8	0,6
0,7	0,0
0,7	0,3
49,1	0,0
3,6	0,0
2,5	0,0
1,4	0,0
5,2	0,0
2,2	0,0
1,5	0,0
20,6	0,1
6,7	0,0
3,1	0,0
1,3	0,2
1,1	0,3
5,5	0,0
3,0	0,1
17,3	0,0

19,6	0,0
66,3	0,0
41,4	0,0
3,5	0,0
2,1	0,0
0,5	0,0
85,4	0,0
82,0	0,0
0,7	0,2
33,5	0,0
11,0	0,0
6,0	0,0
402,2	0,0
235,6	0,0
12,4	0,0
50,6	0,0
42,0	0,1
0,3	0,0
0,2	0,0
0,8	0,2
0,9	0,5
3,6	0,0
0,4	0,1
16,2	0,0
11,3	0,0
4,1	0,0
1,1	0,6
0,0	0,0
3,0	0,0
1,9	0,1
1,8	0,2
8,5	0,0
5,1	0,0
2,3	0,0
0,9	0,4
0,8	0,0
2,0	0,0
8,0	0,0
32,4	0,0
1,0	0,9
124,2	0,0
98,2	0,0
1,2	0,0
9,6	0,0
2,2	0,0
30,9	0,0
14,4	0,0
1,6	0,0
8,4	0,0
2,6	0,0

19,3	0,0
0,9	0,0
0,3	0,0
50,8	0,0
4,3	0,0

Supplementary Table 3. Expressed genes encoding putative plant cell wall degradir
B) Fungal cell wall acting CAZyme encoding genes.

Protein ID	CAZy family	Enzyme
885015	CE4	Chitin deacetylase
815919	CE4	Chitin deacetylase
740302	CE4	Chitin deacetylase
806629	GH5_9	β-1,3-exoglucanase
797080	GH5_9	β-1,3-exoglucanase
795979	GH5_9	β-1,3-exoglucanase
788264	GH5_9	β-1,3-exoglucanase
729515	GH5_9	β-1,3-exoglucanase
885341	GH5_15	β-1,6-endoglucanase
853185	GH16	β-1,3(4)-endoglucanase
274779	GH16	β-1,3(4)-endoglucanase
815608	GH16	β-1,3(4)-endoglucanase
735636	GH16	β-1,3(4)-endoglucanase
791129	GH16	β-1,3(4)-endoglucanase
750894	GH16	β-1,3(4)-endoglucanase
811929	GH16	β-1,3(4)-endoglucanase
741233	GH16	β-1,3-endoglucanase
787504	GH16	β-1,3(4)-endoglucanase
793317	GH16	β-1,3(4)-endoglucanase
791772	GH16	β-1,3(4)-endoglucanase
737176	GH16	β-1,3(4)-endoglucanase
728467	GH16	β-1,3(4)-endoglucanase
357631	GH16	β-1,3(4)-endoglucanase
738853	GH16	β-1,3-endoglucanase
739086	GH16	β-1,3-endoglucanase
790990	GH16	β-1,3(4)-endoglucanase
383381	GH16	β-1,3-endoglucanase
736403	GH16	β-1,3(4)-endoglucanase
791570	GH16	β-1,3(4)-endoglucanase
886936	GH16	licheninase
719041	GH16	licheninase
845840	CBM18-GH16	β-1,3-endoglucanase
814646	GH17	glucan endo-1,3-β-glucosidase
790629	GH17	glucan endo-1,3-β-glucosidase
794017	GH18	chitinase
833274	GH18	chitinase
121758	GH18	chitinase
736277	GH18	chitinase
788648	GH18	chitinase
512857	GH18	chitinase
837441	GH18	chitinase
810847	GH18	chitinase
725953	GH18	chitinase
838588	GH18	chitinase
832557	GH18	chitinase
840055	GH18-CBM5	chitinase
664377	GH18-CBM5	chitinase

17048	GH18-CBM5-CBM	chitinase
437619	GH37	α,α-trehalase
790666	GH37	α,α-trehalase
834199	GH55	β-1,3-endoglucanase
737766	GH55	β-1,3-endoglucanase
791824	GH71	α-1,3-endoglucanase
743565	GH72-CBM43	b-1,3-glucanosyltransglycosylase
749870	GH85	endo-β-N-acetylglucosaminidase
813714	GH128	β-1,3-endoglucanase
791322	GH128	β-1,3-endoglucanase
724588	GH128	β-1,3-endoglucanase
812963	GH131	β-1,3/β-1,6-exoglucanase, β-1,4-endoglucanase
812977	GH131	β-1,3/β-1,6-exoglucanase, β-1,4-endoglucanase

ıg CAZy, central carbon metabolism and fungal cell wall acting CAZy enzymes by *O. rivulosa* grown on

	Time point (FPKM)			
Functional annotation	**2 weeks**	**4 weeks**	**8 weeks**	**4 weeks_over 2 weeks**
Carbohydrate Esterase Family 4 protein	6,1	2,9	5,2	0,5
Carbohydrate Esterase Family 4 protein	443,8	389,0	456,4	0,9
Carbohydrate Esterase Family 4 protein	20,6	24,0	24,7	1,2
Glycoside Hydrolase Family 5 protein	1037,3	40,9	494,8	0,0
Glycoside Hydrolase Family 5 protein	114,5	51,6	68,0	0,5
Glycoside Hydrolase Family 5 protein	214,0	215,7	131,7	1,0
Glycoside Hydrolase Family 5 protein	32,3	41,7	54,5	1,3
Glycoside Hydrolase Family 5 protein	27,4	70,3	143,6	2,6
Glycoside Hydrolase Family 5 protein	98,0	5,3	6,8	0,1
Glycoside Hydrolase Family 16 protein	1035,7	23,0	42,9	0,0
Glycoside Hydrolase Family 16 protein	479,8	20,4	24,1	0,0
Glycoside Hydrolase Family 16 protein	3,6	1,1	1,5	0,3
Glycoside Hydrolase Family 16 protein	124,6	129,4	59,7	1,0
Glycoside Hydrolase Family 16 protein	62,0	86,8	45,0	1,4
Glycoside Hydrolase Family 16 protein	251,4	158,5	194,2	0,6
Glycoside Hydrolase Family 16 protein	3,0	2,7	2,3	0,9
Glycoside Hydrolase Family 16 protein	58,1	59,6	47,6	1,0
Glycoside Hydrolase Family 16 protein	142,2	160,7	133,2	1,1
Glycoside Hydrolase Family 16 protein	517,1	699,5	536,2	1,4
Glycoside Hydrolase Family 16 protein	98,0	187,6	104,0	1,9
Glycoside Hydrolase Family 16 protein	17,1	12,1	19,1	0,7
Glycoside Hydrolase Family 16 protein	12,3	72,5	14,6	5,9
Glycoside Hydrolase Family 16 protein	68,9	119,2	85,1	1,7
Glycoside Hydrolase Family 16 protein	104,0	157,8	137,4	1,5
Glycoside Hydrolase Family 16 protein	602,6	729,5	809,0	1,2
Glycoside Hydrolase Family 16 protein	15,5	27,3	36,0	1,8
Glycoside Hydrolase Family 16 protein	4,0	9,4	10,5	2,3
Glycoside Hydrolase Family 16 protein	1,9	2,6	5,1	1,4
Glycoside Hydrolase Family 16 protein	5,1	13,7	15,8	2,7
Glycoside Hydrolase Family 16 protein	312,4	402,6	338,7	1,3
Glycoside Hydrolase Family 16 protein	93,9	68,2	68,5	0,7
Carbohydrate-Binding Module Family 18 / G	87,3	128,7	127,9	1,5
Glycoside Hydrolase Family 17 protein	161,5	28,4	46,8	0,2
Glycoside Hydrolase Family 17 protein	95,2	182,4	262,7	1,9
Glycoside Hydrolase Family 18 protein	32,9	10,6	5,6	0,3
Glycoside Hydrolase Family 18 protein	104,4	17,1	40,5	0,2
Glycoside Hydrolase Family 18 protein	45,3	16,4	21,2	0,4
Glycoside Hydrolase Family 18 protein	29,6	116,6	17,7	3,9
Glycoside Hydrolase Family 18 protein	42,8	26,2	39,5	0,6
Glycoside Hydrolase Family 18 protein	275,9	339,5	308,0	1,2
Glycoside Hydrolase Family 18 protein	1,9	2,5	2,2	1,3
Glycoside Hydrolase Family 18 protein	438,2	338,6	524,1	0,8
Glycoside Hydrolase Family 18 protein	1,4	2,0	2,0	1,5
Glycoside Hydrolase Family 18 protein	48,5	96,1	180,6	2,0
Glycoside Hydrolase Family 18 protein	1,5	4,3	11,0	2,8
Glycoside Hydrolase Family 18 / Carbohydra	331,9	110,9	111,4	0,3
Glycoside Hydrolase Family 18 / Carbohydra	125,0	54,7	139,5	0,4

Glycoside Hydrolase Family 18 / Carbohydra	143,6	64,8	118,1	0,5
Glycoside Hydrolase Family 37 protein	34,8	7,8	8,8	0,2
Glycoside Hydrolase Family 37 protein	89,8	80,5	112,5	0,9
Glycoside Hydrolase Family 55 protein	1176,6	17,9	37,1	0,0
Glycoside Hydrolase Family 55 protein	167,4	18,9	38,2	0,1
Glycoside Hydrolase Family 71 protein	53,5	58,5	45,2	1,1
Glycoside Hydrolase Family 72 / Carbohydra	184,8	190,7	196,7	1,0
Glycoside Hydrolase Family 85 protein	24,8	18,2	32,0	0,7
Glycoside Hydrolase Family 128 protein	955,2	834,6	616,8	0,9
Glycoside Hydrolase Family 128 protein	191,1	188,8	128,4	1,0
Glycoside Hydrolase Family 128 protein	6,9	12,4	5,0	1,8
Glycoside Hydrolase Family 131 protein	1211,2	78,8	23,8	0,1
Glycoside Hydrolase Family 131 protein	144,5	45,2	33,9	0,3

solid spruce wood during the time course of 8 weeks.

	Comparison			
p-value	**4 weeks_over 8 weeks**	**p-value**	**2 weeks_over 8 weeks**	**p-value**
0,0	0,6	0,0	1,2	0,3
0,0	0,9	0,0	1,0	0,4
0,5	1,0	0,9	0,8	0,0
0,0	0,1	0,1	2,1	0,1
0,0	0,8	0,2	1,7	0,0
0,9	1,6	0,0	1,6	0,0
0,1	0,8	0,1	0,6	0,1
0,0	0,5	0,0	0,2	0,0
0,0	0,8	0,6	14,5	0,0
0,0	0,5	0,0	24,1	0,0
0,0	0,8	0,7	19,9	0,0
0,2	0,7	0,4	2,5	0,3
0,9	2,2	0,1	2,1	0,0
0,0	1,9	0,0	1,4	0,1
0,0	0,8	0,2	1,3	0,1
0,8	1,2	0,7	1,3	0,5
0,8	1,3	0,2	1,2	0,1
0,1	1,2	0,1	1,1	0,0
0,1	1,3	0,3	1,0	0,9
0,0	1,8	0,0	0,9	0,8
0,1	0,6	0,0	0,9	0,4
0,2	5,0	0,2	0,8	0,6
0,0	1,4	0,2	0,8	0,4
0,0	1,1	0,4	0,8	0,2
0,3	0,9	0,7	0,7	0,3
0,0	0,8	0,1	0,4	0,0
0,0	0,9	0,6	0,4	0,0
0,2	0,5	0,0	0,4	0,0
0,0	0,9	0,5	0,3	0,0
0,1	1,2	0,1	0,9	0,2
0,1	1,0	0,7	1,4	0,1
0,1	1,0	1,0	0,7	0,0
0,0	0,6	0,2	3,4	0,0
0,0	0,7	0,1	0,4	0,0
0,1	1,9	0,3	5,9	0,0
0,0	0,4	0,3	2,6	0,1
0,0	0,8	0,1	2,1	0,0
0,1	6,6	0,1	1,7	0,0
0,0	0,7	0,0	1,1	0,4
0,5	1,1	0,7	0,9	0,5
0,5	1,2	0,7	0,9	0,7
0,1	0,6	0,1	0,8	0,1
0,0	1,0	1,0	0,7	0,0
0,1	0,5	0,0	0,3	0,0
0,5	0,4	0,2	0,1	0,0
0,0	1,0	1,0	3,0	0,0
0,0	0,4	0,0	0,9	0,5

0,0	0,5	0,1	1,2	0,2
0,0	0,9	0,5	3,9	0,0
0,5	0,7	0,2	0,8	0,3
0,0	0,5	0,2	31,7	0,0
0,0	0,5	0,1	4,4	0,0
0,4	1,3	0,2	1,2	0,1
0,8	1,0	0,8	0,9	0,6
0,0	0,6	0,0	0,8	0,0
0,1	1,4	0,0	1,5	0,0
0,8	1,5	0,0	1,5	0,0
0,1	2,5	0,1	1,4	0,2
0,0	3,3	0,0	50,8	0,0
0,0	1,3	0,3	4,3	0,0

Supplementary Table 3. Expressed genes encoding putative plant cell wall degrading CAZy, central carbo
C) Central carbon metabolism encoding genes involved in glycosis, mannose catabolism, TCA cycle, L-rha

Protein ID			Time point (FPl	
Glycolysis	Gene	Functional annotation	**2 weeks**	**4 weeks**
789122	*hxk1*	Hexokinase	124,7	129,3
883508	*glk1*	Glucokinase	106,3	57,9
845553	*pgi1*	Glucose-6-phosphate isomerase	405,1	156,5
835136	*pgi2*	Glucose-6-phosphate isomerase	10,4	16,4
839047	*pfk2*	Fructose-2,6-bisphosphatase	455,5	384,9
788402	*pfk2*	ß-D-fructose-2,6-bisphosphate 2-phosphohydrolase	39,9	35,5
830941	*pfk1*	6-Phosphofructokinase 1	40,1	34,2
736978	*fba1*	Fructose-bisphosphate aldolase	506,1	465,8
778449	*tpi1*	Triose-phosphate isomerase	144,1	100,0
812492	*gpd1*	Glyceraldehyde-3-phosphate dehydrogenase	886,4	1085,2
721021	*pgk1*	Phosphoglycerate kinase	250,9	185,9
777519	*pgm1*	Phosphoglycerate mutase (cofactor-independent)	84,7	106,6
816407	*pgm2*	Putative phosphoglycerate mutase	38,7	24,7
732084	*eno1*	Phosphopyruvate hydratase (enolase)	389,2	589,6
794937	*eno2*	Phosphopyruvate hydratase (enolase)	4,7	5,0
884563	*pki1*	Pyruvate kinase	359,8	231,7
786760	*pdc1*	Pyruvate decarboxylase	54,4	141,0
885239	*pdh1*	Pyruvate dehydrogenase complex E1-alpha subunit	176,3	133,0
198505	*pdh2*	Pyruvate dehydrogenase (lipoamide)	139,5	91,9
793545	*acs1*	Putative acetyl-CoA synthase	283,6	267,4
Mannose catabolism				
732619	*pmi1*	Mannose-6-phosphate isomerase	40,8	29,6
811014	*pmm1*	Phosphomannomutase	59,7	63,8
TCA cycle				
813610	*cit2*	ATP: citrate oxaloacetate lyase (mitohodrial) / ATP c	119,6	157,0
788918	*cit1*	Citrate synthase	186,9	208,8
788737	*mcs1*	2-Methylcitrate synthase	186,9	72,1
797053	*aco1*	Aconitase	248,0	301,9
787125	*aco2*	Aconitase	21,4	28,6
729286	*icd1*	Isocitrate dehydrogenase (NADP+)	159,3	75,1
817454	*icd2*	Putative isocitrate dehydrogenase (NAD+)	48,1	51,1
726466	*kgd1*	2-oxoglutarate dehydrogenase (a-ketoglutarate dehydr	116,3	107,7
740166	*kgd2*	2-oxoglutarate dehydrogenase	33,5	20,2
778278	*sdh1*	Succinate dehydrogenase (ubiquinone)	155,9	131,6
778985	*sdh2*	Succinate dehydrogenase (ubiquinone)	132,2	126,0
743296	*fuh1*	Fumarate hydratase (fumarase)	151,1	118,2
776181	*mdh1*	Malate dehydrogenase	835,0	559,6
760258	*mdh2*	Mitochondrial malate dehydrogenase	372,6	205,8
812377	*pcb1*	Pyruvate carboxylase	345,6	355,6
Glyoxylate cycle				
769477	*icl1*	Isocitrate lyase	123,9	335,2
742275	*icl2*	Isocitrate lyase	75,0	65,2
818287	*mas1*	Malate synthase	163,0	246,9
793160	*oxa1*	Oxaloacetase	1332,9	4248,6
810193	*odc1*	Oxalate decarboxylase	114,7	28,7

720584	*odc2*	Oxalate decarboxylase	31,9	38,2
740450	*odc3*	Oxalate decarboxylase	21,8	22,7
823190	*odc4*	Oxalate decarboxylase	0,7	0,6
Leloir				
784856	*gal1*	Galactokinase	53,3	37,1
822974	*gal7*	UTP-hexose-1-phosphate uridylyltransferase (UDP ga	28,8	18,8
834953	*gal10a*	UDP glucose 4-epimerase / UDP-galactose 4-epimera	83,7	85,5
887644	*gal10b*	UDP glucose 4-epimerase / UDP-galactose 4-epimera	22,5	22,1
742665	*ugp1*	UTP-glucose-1-phosphate uridylyltransferase (UDP g	129,5	158,4
839559	*ugp2*	UTP-glucose-1-phosphate uridylyltransferase (UDP g	128,5	326,4
432350	*pgm1*	Phosphoglucomutase	140,1	95,5
L-rhamnose catabolic pathway				
719159	*lra1*	L-rhamnose 1-dehydrogenase	36,2	6,1
750250	*kda1*	L-2-keto-3-deoxyrhamnonate aldolase	186,6	92,4
817972	*kda2*	L-2-keto-3-deoxyrhamnonate aldolase	66,3	43,8
Galacturonic acid catabolic pathway				
765275	*gar1*	Putative D-galacturonic acid reductase	170,2	80,1
794503	*gad1*	L-Galactonate dehydratase	118,0	29,1
807525	*kga1*	Putative 2-keto-3-deoxy-l-galactonate aldolase	382,4	85,6
Pentose catabolic pathway (PCP)				
482062	*lar1*	L-arabinose reductase/Glyceraldehyde reductase	392,2	72,6
811428	*xdh1*	xylitol dehydrogenase	502,6	249,4
830136	*xki1*	Xylulose kinase	146,2	89,1
Pentose phosphate pathway (PPP)				
764085	*rbt1*	Ribulokinase	58,5	41,8
787194	*gnd1*	6-Phosphogluconate dehydrogenase	644,1	470,2
771916	*gnd2*	Phosphogluconate dehydrogenase (decarboxylating)	39,7	35,7
765523	*pgl1*	6-Phosphogluconolactonase	61,5	130,5
791312	*rpi1*	Ribose-5-phosphate isomerase	48,9	46,8
78859	*rpe1*	Ribulose-phosphate 3-epimerase	94,7	50,6
788204	*tkt1*	Transketolase A/Dihydroxyacetone synthase	149,5	115,1
794540	*tal1*	Transaldolase	662,1	302,3
773377	*tal2*	Transaldolase	420,1	360,0
787617	*tal3*	Transaldolase	50,1	48,2
792586	*rbk1*	Ribokinase	12,4	6,7
Trehalose				
722898	*tps1*	Trehalose 6-phosphate synthase (Alpha alpha trehalo	36,5	33,8
819781	*tpp1*	Trehalose phosphatase (Trehalose-6-phosphate phosp	62,7	91,1
437619	*tre1*	Acid trehalase (Alpha, alpha-trehalase)	34,8	7,8
790666	*tre2*	Neutral trehalase	89,8	80,5
809904	*trp1*	Putative trehalose phosphorylase with similarity to Ne	563,3	377,5

n metabolism and fungal cell wall acting CAZy enzymes by *O. rivulosa* grown on solid spruce wood during the mnose, D-galacturonic, Leloir, pentose catabolic and pentose phosphate pathways.

KM)	Comparison				
8 weeks	**4 weeks_over 2 weeks**	**p-value**	**4 weeks_over 8 weeks**	**p-value**	**2 weeks_over 8 weeks**
173,5	1,0	0,0	0,7	0,0	0,7
68,8	0,5	0,7	0,8	0,4	1,5
100,7	0,4	0,0	1,6	0,1	4,0
14,0	1,6	0,1	1,2	0,4	0,7
134,0	0,8	0,1	2,9	0,1	3,4
60,1	0,9	0,0	0,6	0,0	0,7
93,6	0,9	0,1	0,4	0,0	0,4
326,9	0,9	0,2	1,4	0,0	1,5
179,5	0,7	0,0	0,6	0,1	0,8
1359,4	1,2	0,2	0,8	0,2	0,7
246,3	0,7	0,0	0,8	0,0	1,0
153,2	1,3	0,1	0,7	0,0	0,6
35,8	0,6	0,0	0,7	0,1	1,1
898,7	1,5	0,1	0,7	0,1	0,4
6,5	1,1	0,8	0,8	0,1	0,7
534,9	0,6	0,0	0,4	0,0	0,7
131,4	2,6	0,0	1,1	0,7	0,4
277,7	0,8	0,0	0,5	0,0	0,6
198,6	0,7	0,0	0,5	0,0	0,7
239,7	0,9	0,8	1,1	0,7	1,2
50,0	0,7	0,0	0,6	0,0	0,8
149,9	1,1	0,6	0,4	0,1	0,4
204,4	1,3	0,4	0,8	0,5	0,6
215,7	1,1	0,1	1,0	0,7	0,9
148,3	0,4	0,0	0,5	0,1	1,3
267,9	1,2	0,2	1,1	0,4	0,9
28,6	1,3	0,1	1,0	1,0	0,7
119,1	0,5	0,0	0,6	0,1	1,3
89,0	1,1	0,5	0,6	0,0	0,5
106,0	0,9	0,5	1,0	0,9	1,1
46,3	0,6	0,1	0,4	0,0	0,7
219,7	0,8	0,3	0,6	0,2	0,7
169,6	1,0	0,6	0,7	0,2	0,8
121,3	0,8	0,1	1,0	0,9	1,2
713,1	0,7	0,1	0,8	0,3	1,2
280,4	0,6	0,0	0,7	0,2	1,3
358,9	1,0	0,7	1,0	0,9	1,0
104,1	2,7	0,0	3,2	0,1	1,2
88,1	0,9	0,1	0,7	0,0	0,9
91,1	1,5	0,2	2,7	0,1	1,8
1222,2	3,2	0,0	3,5	0,0	1,1
7,0	0,3	0,0	4,1	0,0	16,4

40,7	1,2	0,2	0,9	0,7	0,8
36,1	1,0	0,6	0,6	0,0	0,6
1,2	0,9	0,4	0,5	0,1	0,6
34,8	0,7	0,2	1,1	0,8	1,5
23,8	0,7	0,2	0,8	0,4	1,2
64,8	1,0	0,8	1,3	0,2	1,3
37,4	1,0	0,6	0,6	0,1	0,6
180,7	1,2	0,3	0,9	0,4	0,7
173,3	2,5	0,0	1,9	0,1	0,7
103,2	0,7	0,0	0,9	0,5	1,4
9,9	0,2	0,0	0,6	0,3	3,7
58,7	0,5	0,0	1,6	0,2	3,2
64,5	0,7	0,1	0,7	0,2	1,0
157,7	0,5	0,0	0,5	0,0	1,1
61,5	0,2	0,0	0,5	0,0	1,9
109,5	0,2	0,0	0,8	0,4	3,5
83,2	0,2	0,0	0,9	0,7	4,7
287,0	0,5	0,0	0,9	0,4	1,8
90,2	0,6	0,1	1,0	1,0	1,6
53,3	0,7	0,2	0,8	0,3	1,1
548,7	0,7	0,1	0,9	0,4	1,2
41,7	0,9	0,4	0,9	0,2	1,0
106,8	2,1	0,0	1,2	0,3	0,6
61,5	1,0	0,8	0,8	0,2	0,8
59,1	0,5	0,0	0,9	0,5	1,6
142,6	0,8	0,2	0,8	0,2	1,0
267,1	0,5	0,0	1,1	0,3	2,5
579,8	0,9	0,0	0,6	0,3	0,7
56,1	1,0	0,8	0,9	0,3	0,9
7,0	0,5	0,2	1,0	0,8	1,8
18,9	0,9	0,3	1,8	0,0	1,9
48,3	1,5	0,1	1,9	0,1	1,3
8,8	0,2	0,0	0,9	0,5	3,9
112,5	0,9	0,5	0,7	0,2	0,8
578,5	0,7	0,1	0,7	0,1	1,0

time course of 8 weeks.

p-value

0,1
0,1
0,0
0,2
0,1
0,1
0,0
0,0
0,3
0,0
0,3
0,0
0,1
0,0
0,3
0,1
0,0
0,0
0,0
0,2

0,0
0,1

0,2
0,2
0,3
0,1
0,1
0,1
0,0
0,4
0,1
0,2
0,2
0,2
0,3
0,1
0,6

0,6
0,0
0,0
0,3
0,0

0,2
0,0
0,1

0,0
0,0
0,1
0,1
0,2
0,2
0,0

0,0
0,0
0,9

0,6
0,0
0,0

0,0
0,0
0,0

0,2
0,2
0,5
0,0
0,2
0,0
0,1
0,0
0,0
0,0
0,2

0,0
0,1
0,0
0,3
0,8